Physics – Uspekhi **51** (9) 863 – 885 (2008)

REVIEWS OF TOPICAL PROBLEMS PACS numbers: **61.43. – j**, **61.72. – y**, **62.20. – x**, 81.05.Bx

Synergy effects in the deformation response of thermodynamically open metal – hydrogen systems

L V Spivak

DOI: 10.1070/PU2008v051n09ABEH006506

Contents

Abstract. This paper reviews how polycrystalline and amorphous metals respond to the combined effect of a nonuniform force field and a high-intensity hydrogen (deuterium) diffusion flow. It is shown that deformation effects in such thermodynamically open systems result from phase transitions occurring due to changes in the hydrogen (deuterium) concentration. The necessary and sufficient criteria for observing such synergy effects are formulated. It is shown that the deformation response in a nonuniform stress field is a very sensitive means for indicating first and second-order structural phase transitions in metal – hydrogen systems.

1. Introduction

Various aspects of hydrogen – metal interactions have been an important topic of research by theorists and experimenters over the last 150 years. The current interest in this subject is evidenced by numerous international conferences and symposia devoted to exploring the 'hydrogen' problem and by the ever increasing number of research papers, reviews, and monographs that appear in the literature in this country and abroad [1 – 35]. These works treat such fundamental problems as the hydrogen state in metals and the nature of its abnormally high mobility in iron, palladium, and other metals, as well as the technologically inevitable and frequently undesirable presence of hydrogen in construction materials. To one extent or another, investigations into the reaction of metals to the introduction of hydrogen have implications for the solution to a number of problems facing the atomic power industry, nuclear engineering, and hydrogen energetics.

In the majority of cases, hydrogen is located at interstitial matrix sites of metals and causes virtually no distortion of their crystal lattice. Nevertheless, hydrogen is known to induce stress fields in metals. The strength and the symmetry of these fields depend on the crystal symmetry and the local symmetry of the localization point of a hydrogen atom. It is not a long-range interaction. The deformation interaction energy of hydrogen in alloys is of the order of 0.01 eV [14]. The number of hydrogen atoms is typically smaller than the number of interstitial lattice sites, which accounts for their chaotic distribution over the lattice similar to that of lattice gas atoms. The long-range deformation interaction between introduced atoms increases as the temperature decreases and the hydrogen concentration grows. It allows phase transformations in certain metal – hydrogen ($M-$H) systems, leading to the ordering of such atoms and disintegration of the alloy into domains with significantly different hydrogen concentrations. In the context of a lattice gas model, it is possible to identify phase transitions accompanying the hydrogen redistribution over the lattice of the metal with changes in the aggregate state of the lattice element. From this standpoint, the disintegration process may be interpreted as the condensation of a lattice gas, and the ordering of introduced atoms as crystallization of a lattice liquid. In other words, variations in the temperature and concentration in the $M-$H system may induce gas $\leftrightarrow$ liquid $\leftrightarrow$ solid phase transitions.

Both the diversity of phase transitions in $M-$H systems and the high hydrogen mobility in certain transition metals can be used to develop model systems for the study of various phenomena in solids that occur both in a closed thermodynamic system during phase transitions caused by tempera-

L V Spivak Perm State University,
ul. Bukireva 15, 614990 Perm, Russian Federation
Tel. (7-342) 239 63 83
E-mail: lspivak@psu.ru

Received 24 October 2007, revised 30 April 2008
Uspekhi Fizicheskikh Nauk **178** (9) 897 – 922 (2008)
DOI: 10.3367/UFNr.0178.200809a.0897
Translated by Yu V Morozov; edited by A M Semikhatov

ture variation and in an open thermodynamic system exchanging mass and energy with the ambient medium. In the latter case, phase transitions can be initiated only by changes in the hydrogen concentration in the $M-H$ system. A distinct feature of these phase transitions is that they develop only in the 'hydrogen' sublattice, whereas the distribution of atoms in the metal sublattice remains virtually unaltered. This may be partly accounted for by the fact that hydrogen diffusion coefficients are many orders of magnitude greater than self-diffusion coefficients of metal atoms and components with which they form solid solutions. Hence, there is a fundamental difference between the behavior of other interstitial alloys ($M-O$, $M-N$, $M-C$, etc.) and that of $M-H$ alloys.

This field of knowledge was long dominated by applying a stereotype approach to the study of $M-H$ alloys, in which processes of active metal saturation with hydrogen were considered separately from its effect on the properties of alloys, including mechanical properties. This means that the consequences of introducing hydrogen into metals were actually assessed in thermodynamic equilibrium. But it is well known that the high diffusibility of hydrogen atoms in certain transition metals creates conditions under which the introduction of hydrogen originally induces a well-apparent response of the metal; in many cases, a dramatic scenario of the active phase of hydrogen-matrix interactions develops directly in the course of hydrogen saturation of the metal and sometimes continues long after hydrogenation is terminated.

Accomplishment of the main task, i.e., *in situ* evaluation of the response of metals and alloys to the introduction of hydrogen, encountered experimental difficulties attributable to the absence of instrumental methods for the study of $M-H$ interactions during hydrogen introduction directly into the metal's matrix from the gas phase or electrolyte. This especially refers to structural studies. Naturally, emphasis has been given to the consideration of matter characteristics such as the internal friction, electric resistance, and mechanical after-effect, which are most vulnerable to structural changes. Surprisingly, the deformation response to hydrogen introduction into metals proved to be especially easy to record and measure with a high degree of accuracy and reproducibility. Specifically, the available data indicate that mechanical after-effects and their consequences may be of special importance for the solution to many problems due to the high informativity and susceptibility of these effects to structural-phase changes.

We note that early studies of iron and iron-based alloy responses to the introduction of hydrogen at the stage of active plastic strain were driven by technological applications. A group of researchers headed by Karpenko was the first to address this issue [1]. Studies of this kind may be described as the analysis of hydrogen action at different stages of plastic flow in metals under 'tough' loading conditions (e.g., at a stress $\sigma = f(\varepsilon, \dot{\varepsilon})$, where ε and $\dot{\varepsilon}$ are the strain magnitude and rate), also called 'dynamic' saturation of metals with hydrogen. Such loads are usually much greater than the macroscopic flow limit.

Important data on the dynamic hydrogen saturation (HS) in pure and superpure iron ($RRR_H \sim 6000$, where RRR is the residual resistivity ratio) were obtained from 1970 to 1990 by researchers at Tokyo University (S Asano, R Otsuka, Y Kimura, H Matsui et al.), the Polish Academy of Sciences (M Smialowski, J Flis, E Lunarska, et al.), and the University of Illinois (H Birnbaum, T Tabata et al.) [36 – 50]. The very first comprehensive analysis of these works can be found in publications by E A Savchenkov, M M Shved, J Hirth, and other authors [12, 17, 22, 26].

We emphasize that the first reports on the combined effect of stress fields and HS on other metals (e.g., Va metals and palladium, which interact with hydrogen as actively as iron does) were published quite recently.

Because most construction materials are designed to be used at roughly 300 K, hydrogen is introduced electrolitically, using the sample being saturated with hydrogen as the cathode, the platinum lattice as the anode, and aqueous solutions of sulfuric acid or alkalies as electrolytes; organic compounds are used when metals are hydrogenated at negative temperatures. It is important that electrolytic saturation permits reaching an atomic hydrogen pressure at the metal surface equivalent to 1000 atm at the cathode current density $i_c = 1000$ A m^{-2} (see Ref. [6]). The modified Sieverts law, stating that the amount of hydrogen introduced into a metal is proportional to $i_c^{1/2}$ (all other conditions being equal), remains valid in a wide range of cathode current values [51 – 53].

Analysis of published experimental data has revealed marked discrepancies between results obtained by different research groups even for iron samples of similar composition. This makes the interpretation of the mechanical behavior of metals difficult. The discrepancy is due to several causes. One is the different compositions of electrolytes. Most authors report neither the characteristics of the sample surface nor the formation of oxide or other films that may substantially restrict the inflow of hydrogen into the metal even under constant conditions (temperature, electrolyte composition, cathode current density, etc.). Other contributors to the discrepancy are differences in the sample size and geometry, strain rate, etc.

One more circumstance complicating the interpretation of experimental results is the uncertainty arising from the fact that a change in the metal structure during 'dynamic' HS due to plastic strain is associated with a change of its state caused by the introduction of hydrogen. Such a test scheme (the 'stiff' mechanical testing scheme) makes it difficult to detect those structural changes that are specifically related to the action of hydrogen.

Another version of the test, the so-called 'mild' loading scheme of evaluating mechanical after-effects, appears to be more advantageous. It treats strain as a response to the applied stress, which is normally much weaker than the macroscopic flow limit of a given material (quasielastic loading).

However, only the measurement of internal friction is currently used in the studies of $M-H$ systems. Evidently, it cannot be the sole source of information on the nature of hydrogen interactions with metals in the presence of static (or other) external and internal stress fields.

In the ideological context, narrowing the scope of research to the joint action of stress fields and the hydrogen diffusion flow on iron and iron-based alloys reduced the theory of this deformation response to a rather trivial dislocation paradigm (neither hydride phases nor the associated phase transformations of a different type have been found in iron under normal conditions). Some researchers argue that the interaction of hydrogen with dislocations restricts their motion and facilitates degradation of the plastic properties of metals; others believe that such interactions contribute to the dislocation

mobility and to a lower flow stress. Neither approach differentiates between the behavior of $M-H$ alloys having the established composition (closed thermodynamic systems) and in the course of active interaction of iron with hydrogen.

Clearly, further progress in understanding the behavior of such thermodynamic systems is difficult, if not impossible, without studying metals and alloys with the hydrogen diffusion coefficient at 300 K close to that in iron and their response to the direct introduction of hydrogen and subsequent relaxation processes.

In the 1980s, some authors reported a marked amplification of strain and an increased rate of direct and reverse mechanical after-effects as a result of the hydrogenation of iron undergoing torsional strain [54–59]. These observations became the starting point for a series of research on the response (including the deformation response) of hydrogen-saturated iron, palladium, Va metals, zirconium, TiNi intermetalloids, and amorphous alloys based on iron, nickel, cobalt, and other metals and alloys.

These studies laid the foundation of a new field of research combining two interrelated aspects of hydrogen interaction with crystalline and amorphous metals — the behavior of metals and alloys in the course of saturation with hydrogen (open thermodynamic $M-H$ systems) and during the transition to a thermodynamically more stable state. The last aspect implies follow-up investigations into the structure and properties of metals and alloys long after their hydrogenation and the behavior of such alloys during thermocycling and after it.

The present retrospective review covers previous studies on the synergistic behavior of metals during intense hydrogenation and the concomitant action of stress fields. The term 'synergistic' is derived from the Greek word 'synergy' meaning working together; it is used to describe a situation where the final outcome of concerted action of individual factors is much greater than the naive sum of its parts.

Indeed, loading metals below the elasticity limit results in a weak deformation governed by the Hooke law. If a metal is saturated with hydrogen in the absence of external or internal stress fields, all deformation effects are reduced to volumetric changes, relatively weak and undirected. If a load below the elastic limit is applied to a preliminarily hydrogenated metal, the strains are equally small and obey the Hooke law. Only the combined action of a stress field and a hydrogen diffusion flow causes deformations an order of magnitude stronger than those developing under the effect of either factor.

Although the synergy effects of microplasticity in hydrogen–metal interactions were first observed in iron, it seems appropriate to begin the discussion from the studies of metals of the Va subgroup because they most clearly expose the main properties inherent in all $M-H$ systems. Consideration usually involves a triad of mechanical after-effects: creep or an direct after-effect characterized by a constant applied stress; relaxation of stress causing a fixed macroscopic strain; and the reverse mechanical after-effect, i.e., spontaneous deformation of metals after their plastic strain and unloading.

2. Transformation plasticity effects in the hydrogen saturation of the subgroup of Va metals and zirconium

In terms of the interaction with hydrogen, metals comprising the Va subgroup (vanadium, niobium, and tantalum) have in common rather high (of the order of $10^{-9}-10^{-10}$ m^2 s^{-1}) hydrogen diffusion coefficients at 300 K [13, 15], a single type of crystal lattice (BBC lattice), the formation of the hydride β-phase by hydrogen atom ordering in the matrix crystal lattice, the diffusion-cooperative shearing character of hydride crystal nucleation, and growth at the stage of the two-phase $(\alpha+\beta)$ state.

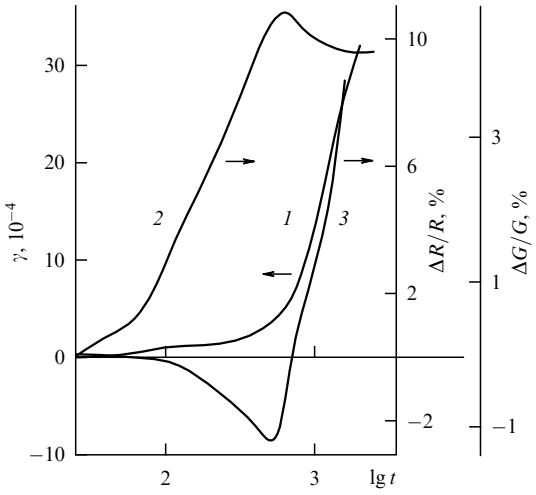

Figure 1. The effect of the duration of vanadium saturation with hydrogen on the creep strain γ (*1*), variation in the electric resistance R (*2*), and the shear modulus G (*3*) ($i_c = 250$ A m^{-2}, $\tau = 25$ MPa, time t in seconds).

When a torque is applied to a sample of Va metals to create tangential stress in the surface level $\tau < \tau_s$, where τ_s is the flow limit, it is impossible to measure creep with an accuracy of 10^{-7}. At the same time, hydrogenation of recrystallized (i.e., lacking internal stresses) samples in the absence of an external stress field does not lead to apparent deformation either. But the combined action of a stress field and a hydrogen diffusion flow produces a manifold increase in the creep rate and magnitude. This is called the synergistic effect of the deformation response during hydrogen saturation of metals.

A similar situation occurs in hydrogen-induced stress relaxation and reverse mechanical after-effects [26, 60–75].

Characteristic dependences of the creep strain activated by a hydrogen diffusion flow and of reverse mechanical after-effects are shown in Figs 1–3 for vanadium, the most typical metal with the set of properties listed above.

The creep strain at loading below the flow limit and HS may be as strong as 10^{-3}, i.e., may have a macroscopic value (see Fig. 1).

Creep initiated by hydrogenation (hydrogen-initiated direct mechanical after-effect, HDMA) has the following kinematic characteristics. First, there is a certain period (t^*) of hydrogen saturation during which the strain is relatively weak (inertness period), in fact practically arrested when the saturation is discontinued. Also, an increase in the cathode current density i_c or magnitude of the applied stress τ inevitably reduces the time t^* after which such a deformation is activated.

It was shown (see Fig. 1) that HDMA becomes apparent as soon as the maximum electric resistance of the metal is reached, i.e., from the onset of precipitation of the second, β-hydride phase, from the α-solid solution of hydrogen, as

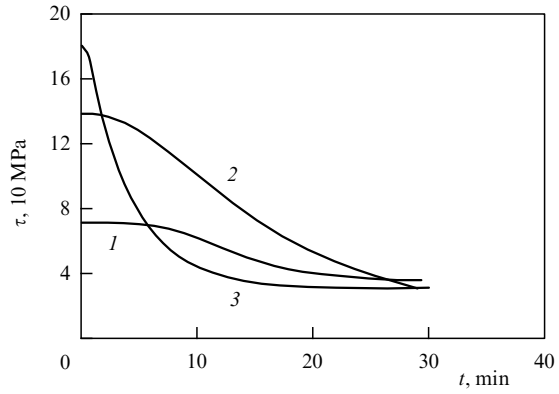

Figure 2. The effect of duration of vanadium saturation with hydrogen on stress relaxation: *1–3*, different levels of initial stresses τ_0. ($i_c = 250$ A m^{-2}.)

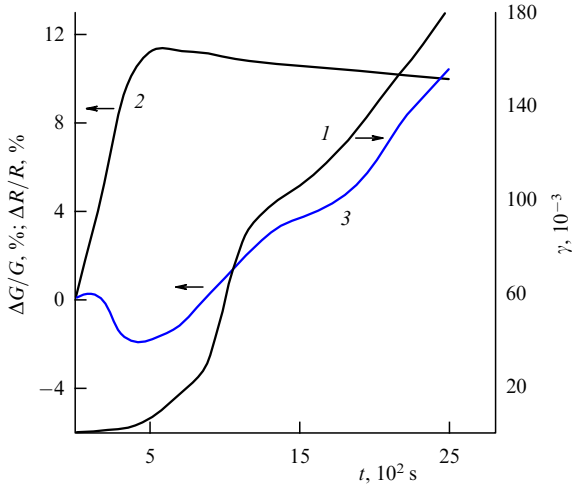

Figure 3. The effect of the duration of vanadium saturation with hydrogen on RMA (*1*), variation of the electric resistance (*2*), and the shear modulus (*3*). ($i_c = 250$ A m^{-2}, $\gamma_t = 0.4$.)

confirmed by X-ray structure analysis (RSA) and changes in the shear modulus (see also Refs [64, 74]).

In such experiments, the strain rate gradually increases parallel to the increasing duration of hydrogenation. Deformation continues until the metal disintegrates. As the applied load τ ($\tau < \tau_s$) increases, the creep magnitude and rate also increase. The time necessary for the degradation decreases almost linearly with increasing τ and $i_c^{1/2}$. It is noteworthy that the peaking of the electric resistance curve $\Delta R/R(t)$, i.e., the time during which the limit concentration of hydrogen in the α-phase is reached, also decreases in proportion to $i_c^{1/2}$.

It is maintained in Refs [51–53] that the amount of hydrogen electrolytically introduced into a metal is proportional to $i_c^{1/2}$. This means that the creep strain activation during hydrogen saturation of Va metals starts only after the hydrogen concentration increases to a certain level above which hydride phases begin to precipitate from the α-phase, i.e., after the onset of the phase transition. The time necessary to reach such a concentration depends on the saturation intensity. In other words, the deformation accompanying hydrogenation of metals, e.g., vanadium, in an external stress field is nothing but a specific manifestation of the transformation plasticity effect (TPE).

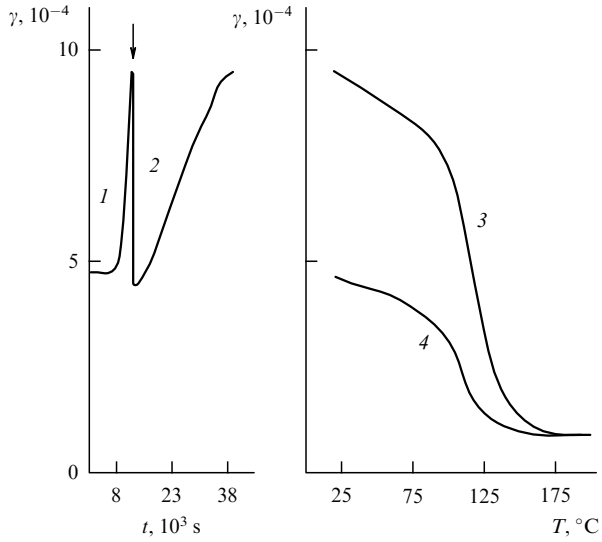

Figure 4. The effect of the duration of vanadium saturation with hydrogen under load (*1*) or without it (*2*) and of subsequent thermocycling (*3*, heating; *4*, cooling) on metal deformation ($i_c = 250$ A m^{-2}, $\tau = 50$ MPa). ↓ denotes unloading of the sample (*2*).

Eliminating the stress field and heating the sample after the hydrogenation give rise to a strain whose the direction is opposite to that of the strain in an alloy hydrogenated in an external stress field. In vanadium, the strain recoverable upon heating is practically identical with the strain accumulated in the active phase of saturation in the creep regime. In niobium, the strain recoverable upon heating is smaller than that accumulated in the HDMA regime. Tantalum is intermediate in this respect. The greater τ, i_c, and the duration of saturation, the stronger such deformation. It is essential that heating arrests the strain evolution at the temperature necessary for complete dissolution of hydride phases and the formation of a homogeneous α-phase as shown by direct and indirect analysis of the alloy structure. Thus, in the given loading diagram, the primary mechanism of hydrogen-induced creep is the oriented growth of hydride species coordinated with the loading path.

Weighty evidence of TPE due to the oriented growth of new phase precipitates was given by the observation of oriented transformation strain (OTS). OTS in classical shape-memory alloys (SMAs) is described as follows [76–79]: if a sample is unloaded at a certain cooling stage in a temperature range suitable for the thermoelastic martensitic transformation, its deformation continues in the same direction upon further cooling or isothermal holding. Under usual conditions, OTS occurs due to the directed growth of thermoelastic martensite crystals whose orientation is set at the previous cooling stage by stress fields acting on the sample. Among a large number of alloys likely to display the shape memory (SM) effect, only Cu and Fe-doped TiNi intermetallide, CuMn alloys [76–79], and a few other systems have been shown to undergo OTS.

Precipitation and growth of vanadium hydrides is a crystallographically ordered process [13, 14, 80–85]. The presence of OTS in V–H alloys could be expected, bearing in mind peculiarities of the crystallographic phase relation and the small bulk effect of hydride transformation. The results of numerous experiments have confirmed this conjecture (Fig. 4). Hydrogenation of a vanadium sample after

unloading is conducive to the continuation of active deformation even though its rate naturally becomes somewhat lower than under loading because the orienting external stress field is absent. Continuation of the deformation is most likely due to the growth of properly oriented hydride phase crystals formed at the preceding stage and to the nucleation and growth of new precipitates. Their orientation is governed by the internal stress field arising from a spatial distribution of the previously formed hydride precipitates. Taken together, a large number of such shifts cause macroscopic strain. We note that in this experimental design, subsequent heating also almost totally recovers the strain (curve *3* in Fig. 4) accumulated during hydrogen saturation under load and without it.

The results of these experiments are regarded as strong evidence of coordination between the growth direction of hydride crystals and the loading path during hydrogenation of Va metals.

We emphasize that OTS in the hydrogen saturation of metals is essentially different from OTS observed in [76–79]. In Refs [76–79], OTS occurred in the situation of coherent growth of new-phase crystals crystallographically ordered with respect to the matrix when all diffusion processes were forbidden. In the present case, active hydrogen diffusion was a necessary condition for the observation of OTS. In the former situation, OTS occurred upon varying the temperature of alloys having an established composition; in the latter case, OTS developed as the alloy composition changed at a constant temperature, i.e., when the OTS concentration effect was apparent.

As shown in the papers cited above, the onset of deformation in the HDMA regime is associated with the emergence of new phases. This gives a reason to expect a significant increase in the time t^* for those Va metals that have a wider range of existence of homogeneous solid α-solutions, e.g., for a Ta–H system [14, 81–85]. Such an increase has been observed in experiments.

Evidently, the absence of well-apparent OTS in Nb–H alloys may be due to the relatively small β-phase tetragonality (0.001) despite the well-defined crystallographic relations between β-phase crystals and the matrix phase and the formation of the β-phase by the martensitic mechanism. On the other hand, the disorienting influence of the strong bulk effect of hydride (β) transformation in this system cannot be disregarded.

Traditionally, only one loading path is considered in TPE studies (the behavior of a material under constant external loading), although TPE also occurs at other loading regimes, e.g., in stress relaxation or a reverse mechanical after-effect (in other words, when a phase transition occurs in a stress field, either internal or external).

Stress relaxation (SR) is understood [86] as a spontaneous time-dependent decrease in stress needed to maintain the permanent macroscopic strain. Typically, stress relaxation in metals is due to the transition from elastic strain to plastic strain [86].

When a torque creating a surface stress $\tau_0 < \tau_s$ is applied to vanadium, tantalum, or niobium samples, stress relaxation is negligibly small and is completed very quickly (usually within a few minutes or sooner at 300 K), considering a 'mild' loading diagram is used.

Saturation of a metal with hydrogen under SR conditions substantially accelerates this process (see Fig. 2). In such experiments, SR has one important feature: the applied stresses abate with time not spontaneously but in the course of hydrogen penetration into the metal. In fact, this process should be described as quasirelaxation. In what follows, by SR in a sample undergoing hydrogenation, we mean 'hydrogen-initiated stress relaxation (HSR).'

As in the case of HDMA, HSR in Va metals begins to develop after a lag-time (t^*) that is the smaller, the bigger is the starting load τ_0 (see Fig. 2) and the higher is the cathode current density i_c. All other conditions being equal, the length of such an inertness period depends on the chemical nature of the metal undergoing saturation, the hydrogen diffusion coefficient in this metal, and the concentration field of the homogeneous solid solution. It was shown in structural and other studies that in this case too, relaxation processes are activated after a certain amount of the hydride phase forms in near-surface volumes of the sample. Thus, transition from an elastic strain to a plastic one (responsible for a reduced τ) occurs in the process of hydride transformation during saturation of a given metal with hydrogen, i.e., first and foremost due to TPE.

In most cases, a straightforward approximation permits describing the behavior of these metals under different saturation conditions by an equation of the type

$$\Delta\tau(t) = \alpha^* \ln(\lambda t + 1) \tag{1}$$

with

$$\alpha^* = \frac{kT}{V^*},$$

where $\Delta\tau = \tau_0 - \tau$, V^* is the apparent activation volume, k is the Boltzmann constant, and λ is a constant. Formula (1) was used to estimate some activation parameters of the process.

It was found that τ_0 tends to decrease with increasing V^*. Calculations showed that for $\tau_0 < \tau_s$, the apparent activation volume is $V^* = (60-250) \times 10^{-24}$ cm^3 for vanadium, $V^* = (50-340) \times 10^{-24}$ cm^3 for tantalum, and $V^* = (70-230) \times 10^{-24}$ cm^3 for niobium. These values are much smaller than V^* characteristic of dislocation SR mechanisms proper (see Refs [87–91]) ($V^* \sim 10^{-18}-10^{-20}$ cm^3) but become greater than or (as τ increases) closer to the local volume V^* in which an elementary act of hydrogen diffusion occurs [$V_0 \sim (30-40) \times 10^{-24}$ cm^3]. As $\tau_0 \to \tau_s$, $V^* \to V_0$. Thus, the HSR rate and magnitude are determined by the initial value of τ_0, the metal structure, the type and crystallographic characteristics of hydride precipitates, the hydrogen saturation conditions, and the diffusion characteristics.

The functional relation between the duration of the incubation period, the cathode current density, and the applied stress can be represented as

$$\ln t^* = \text{const}\,(i_c^*)^{-1/2}\tau_0^{-1}\left(\sqrt{\frac{i_c^*}{i_c}} - 1\right), \tag{2}$$

where i_c^* is another constant, whose physical meaning is that of the cathode current density at which HSR begins practically immediately after the onset of saturation.

The dependence $t^*(i_c)$ suggests an important role of power-diffusion processes in HSR. We suppose that $i_c = 0$ (no hydrogen is introduced into a metal). For $\tau_0 < \tau_s$ and $\tau_0 = \text{const}$, $t^* \to \infty$, HSR is then absent. If $i_c \to i_c^*$, then $t^* \to 0$; in other words, the incubation period is very short when the current density equals i_c^*. If $i_c = \text{const}$, $\tau_0 = 0$, then $t^* \to \infty$.

Thus, it follows from (2) that HSR can be observed if both an intensive hydrogen flow through the metal crystal lattice ($i_c > 0$) and a stress field ($\tau > 0$) are present. Fulfillment of these two conditions leads to the synergistic effect. This explains why HSR is observed only in metals with large enough hydrogen diffusion coefficients at 300 K.

Heating of the sample after HSR produces a well-apparent (of the order 10^{-3}) strain directed opposite to the strain during HSR. The bigger τ_0 and i_c and the longer the duration of hydrogen saturation, the greater such strain is. It is essential that the strain discontinues after the complete dissolution of hydride phases and the formation of a homogeneous α-phase. These findings agree with the results of HDMA studies and indicate that in the present loading scheme, the oriented growth of hydride species coordinated with the loading is also the principal mechanism of hydrogen-induced HSR.

By the reverse mechanical after-effect (RMA), we mean spontaneous strain in a plastically deformed metal following the withdrawal of the deforming force. In the general case, the driving force of this process is the relaxation of internal stresses induced by plastic strain. Normally, the maximum value of this strain in the metals being considered does not exceed 10^{-5}.

However, the saturation of vanadium, tantalum, and niobium with hydrogen may activate the strain γ to $10^{-3}-10^{-2}$. The typical time dependence of hydrogen-induced RMA, $\gamma(t)$, is presented in Fig. 3. A characteristic feature of the Va metal behavior under these loading conditions is the incubation period of the length t^*. This period shortens as the degree of preliminary torsional strain γ_t and i_c increases and, for constant γ_t values, is roughly proportional to $i_c^{-1/2}$. RMA stops when polarization current is switched off (i.e., when hydrogen saturation terminates).

As in HDMA and HSR, the onset of active RMA and its further development roughly coincide with the nucleation and growth of hydride species. X-ray diffraction studies indicate that inflections of the $\gamma(t)$ curves are due to the emergence of new hydride phases in the solid solution characterized by specific crystallogeometry, the bulk transformation effect, and other properties. Most probably, the transformation of the alloy structure during saturation with hydrogen proceeds as

$$\alpha \rightarrow \alpha + \alpha' \rightarrow \alpha + \alpha' + \beta \rightarrow \alpha + \beta\,,$$

where α' is a hydrogen-enriched domain of the solid solution that arose from its layering into hydrogen-depleted and hydrogen-rich microvolumes (spinodal decomposition). In the bulk, this phase transition chain is observed only in the hydrogenation of niobium and, to a lesser degree, in vanadium. Tantalum is intermediate in this respect.

To summarize, hydrogenation in this stress state scheme activates RMA only when the hydrogen concentration in near-surface volumes is close to the value at which the α-phase can exist.

In all cases without exception, heating of hydrogenated SMA in the RMA regime causes strain with the sign opposite to that of the strain that develops in a metal undergoing saturation with hydrogen in a stress field. All other conditions being equal, the greater the degree of hydride phase tetragonality and the smaller the bulk effect of hydride transformation, the more apparent is the strain return during heating of Va metals hydrogen-saturated in an internal stress field.

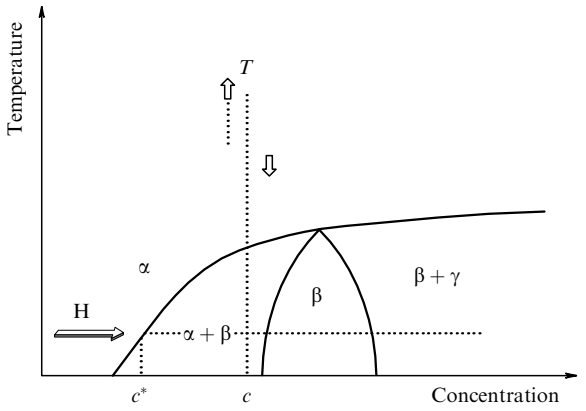

Figure 5. Different modes of realization of the transformation plasticity effect and the shape memory effect in an alloy with the established composition at varying temperatures, and hydrogen concentrations, and at a constant temperature (diagram).

Thus, strains produced by the joint action of an external (or internal) stress field and a diffuse hydrogen flow in metals of the Va subgroup (vanadium, niobium, and tantalum) are associated with hydride phase transformation of the diffusion-cooperative type proceeding under strongly nonequilibrium hydrogenation conditions.

In this situation, unlike in traditional TPE experiments where transition from one phase state to another in an alloy of constant composition is due to a change in the temperature, the unusually high diffusibility of hydrogen at 300 K allows observing TPE in isothermal conditions. Phase transitions are activated (see Fig. 5) by an increase in the hydrogen concentration in a metal and result from the nucleation and growth of hydride species. Conditions necessary and sufficient for observation of TPE during hydrogenation are the existence of a nonuniform stress field, a high diffusion mobility of hydrogen atoms (the diffusion coefficient at 300 K at least $10^{-11}\,m^2\,s^{-1}$), and the presence of hydride phases on the $M-H$ state diagram that arise through the mechanism of hydrogen atom ordering in the matrix crystal lattice with the formation of the hydrogen's own sublattice.

Elucidation of conditions necessary and sufficient for the observation of synergistic effects of microplasticity in Va metal – hydrogen systems provided a basis for the search for other systems where similar effects can be expected. In this context, the behavior of zirconium appeared enigmatic. On the one hand, it was shown in [92] that heating Zr – H alloys containing hydride compounds (Zr_2H and possibly ZrH) after plastic strain or holding them at a high temperature in the presence of a stress field leads to the hydride crystal reorientation in conformity with the stress-state pattern. Such behavior somewhat resembles that of Va metals. On the other hand, the hydrogen diffusion coefficient in zirconium at 300 K is negligibly small [93]; this violates one of the conditions for the manifestation of synergistic effects of microplasticity under the joint action of a hydrogen diffusion flow and a stress field formulated based on the results of vanadium, tantalum, and niobium experiments

As shown experimentally in [94, 95], loading zirconium samples below the macroscopic flow limit ($\tau = 0.8\tau_s$ or 290 MPa) and their subsequent hydrogenation result in a strong nonmonotonically developing strain (Fig. 6). The onset of activation of the deformation process coincides with the precipitation of the hydride phase from the α-solid

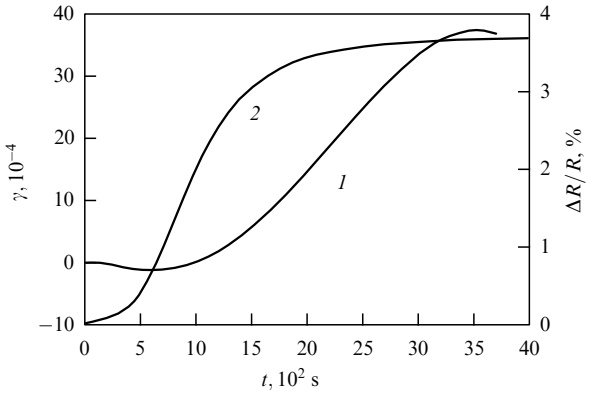

Figure 6. The effect of the duration of zirconium saturation with hydrogen on the creep strain at $\tau = 290$ MPa (*1*), change in the electric resistance (*2*) ($i_c = 350$ A m^{-2}).

solution of hydrogen in zirconium, as evidenced by the slow incremental increase in the electric resistance and the alternating sign of dR/dt and dG/dt derivatives on the $R(t)$ and $G(t)$ curves.

It is noteworthy that zirconium behavior in the creep regime during hydrogenation fairly well correlates with the behavior of niobium observed in earlier studies [63]. Treatment of zirconium with hydrogen in a stress field causes substantial (in terms of rate and magnitude) HDMA only close to the biphasicity limit and when the hydride transformation (i.e., the hydride phase transition) develops. This finding suggests that the observed strain acceleration is a manifestation of the concentration-dependent transformation plasticity effect arising exclusively from isothermal variation of the hydrogen concentration [26, 68]. The resulting strain can be regarded as a sum of microscopic shifts (distortions) that develop when hydride crystals grow in a stress field via the bainitic mechanism [68, 89].

Similarly to Va metals, the heating of hydrogen-saturated zirconium induces strain with the opposite sign. In this case, a peculiar manifestation of the SM effect is observed (see Refs [26, 62, 68]). Cooling naturally causes a much weaker strain, although greater than the resolving power of the method. The presence of a small cooling-induced strain suggests precipitation of part of the hydride phase at sites where it was initially present; these hydride species retain the orientation they had after hydrogenation (prior to heating).

In full conformity with V, Nb, and Ta experiments, the introduction of hydrogen into plastically strained zirconium (RMA regime) accelerated RMA and induced a multiply reversible SM effect. This means that hydrogenation of both Va metals and zirconium in an external or internal stress field triggered deformation processes that did not develop under loading without hydrogenation or under loading of previously saturated samples.

A strong bulk effect of hydride transformation in a Zr–H system estimated at $\sim 14\%$ [85] accounts for the appearance of epitaxial dislocations during the growth of hydride β-phase crystals in the case of disturbed coherence of the matrix coupling. The concentration of dislocations at sites occupied by hydride particles after their dissolution upon heating facilitates the effect of subsequent cooling (α-phase dissociation) on the precipitation of hydride species of the same size and orientation that they had in these local regions of the matrix before heating. Additional factors contributing to 'freezing' the original orientational states in plastically strained samples are the internal stress fields remaining after heating zirconium below the polygonization and recrystallization temperatures, as is the case with classical SMA, e.g., nitinols [77, 78].

A study of the deformation response in zirconium demonstrated that the extrapolation of the results of high-temperature measurements of the hydrogen diffusion coefficient is invalid in a lower-temperature region. One explanation is the altered mechanism of hydrogen diffusion in the crystal lattice of zirconium, that is, transition of the suprabarrier mechanism operating at high temperatures to thermally activated tunneling [25] at lower temperatures. This is one more example illustrating the high sensitivity of the deformation response to structural-phase transformations in $M-H$ systems.

The high susceptibility of mechanical after-effects to phase, primarily hydride, transformations was previously noted in Ref. [96].

Analysis of experimental data on TPE in Va metals and zirconium shows that deformation typically starts to develop shortly before the α-phase concentration limit is reached. Results of X-ray studies and especially shear modulus measurements suggest the existence of a certain subtransient state preceding the precipitation of an M_2H-like stable hydride phase. Regardless of the shape of the stable $M-H$ state diagram, this subtransient state is identified with the emergence of hydrogen-poor (α) and hydrogen-rich (α′) phases as a result of stratification of the homogeneous α-solid solution, i.e., with the transition $\alpha \rightarrow \alpha + \alpha'$ (spinodal decomposition).

In principle, all stable $M-H$ diagrams (V, Na, Nb, Zr) contain regions of such transformations in some temperature and concentration range [14]. For electrolytic hydrogen saturation, their probability is always high, at 300 K, in particular. Thereafter, the hydride β-phase is precipitated at the α′-phase as a substrate [13, 14].

As the spinodal decomposition interval ($\alpha \rightarrow \alpha + \alpha'$) was passed under load in [26], strains were apparent not only after cooling below the critical point; reverse heating (even under loading) also recovered strains accumulated after cooling in the ($\alpha + \alpha'$)-region. The theory of spinodal decomposition implies generation of concentration waves as regions with high and relatively low concentrations of one of the components (e.g., hydrogen) alternating within a single structural state. Singularity of these effects and the lack of references to them in the literature on spinodal decay in alloys necessitated a thorough analysis of this phenomenon, most of all the evaluation of the possibility of observing such strains in principle [97]. In the model under consideration, the hydrogen-rich region (an asymmetric hydrogen cluster) is regarded as the elementary structural unit oriented in the stress field created by torsional strain, which accounts for the biaxiality of the medium. A few assumptions simplify the expression for the strain tensor U_{ik} to the final form

$$U_{ik} = \frac{1}{2\mu}\,\sigma_{ik} + n\gamma\eta_{ik}\,, \qquad (3)$$

where σ_{ik} is the torsional stress tensor, μ is the shear modulus, n is the number of clusters per unit volume, η_{ik} is the biaxial strain tensor, and γ is the parameter characterizing the response of the cluster system to the applied field (a phenomenological parameter derived from the experimental one). The results of numerical calculations indicate that

application of a certain dimensionless torsional stress to a system passing the critical temperature induces a deformation response reversible upon heating. The response is absent if the temperature is higher than the spinodal decay temperature.

3. Transformation plasticity effects in the hydrogen saturation of palladium

The conclusions drawn in the preceding section cannot be regarded as objective without a similar analysis of Pd–H systems, which in many respects satisfy conditions necessary for observing synergic effects. Suffice it to say that hydrogen in palladium has a rather high diffusion coefficient at 300 K, the hydride phase arises from the ordering of hydrogen atoms in the matrix crystal lattice, and the hydride phase is produced by the spinal mechanism (as in niobium) with the formation of hydrogen-poor and hydrogen-rich regions in the matrix. But the crystallographically ordered character of hydride-phase precipitates in palladium is not as well apparent as in Va metals and zirconium, even though the results of some recent experiments [98] appear to confirm it (see also Ref. [29]).

The creep strain of palladium in the absence of hydrogen ($T = 300$ K, $\tau < \tau_s$) does not exceed 2×10^{-6} for ~ 60 min (period of observation). The introduction of hydrogen [26, 99–101] markedly accelerates the creep, and HDMA amounts to 2×10^{-3} during the same time (Fig. 7). This phenomenon is essentially different from the so-called hydrogen elasticity [102–105].

In the absence of hydrogen, SR in palladium is negligibly small and practically completed within a few minutes of isothermal holding, the degree of SR, τ^*/τ_0, being 0.98 (τ_0 and τ^* are the initial and final stresses, respectively). The situation changes dramatically if an elastically strained palladium sample is treated with hydrogen. As shown in Fig. 7, the rate of HSR increases by several orders of magnitude and a practically complete SR is achieved within 60–70 min of saturation ($i_c = 500$ A m^{-2}). The maximum rate of the process is reached, as in Va metals, only some time after the onset of hydrogenation.

It is shown that i_c has a weak effect on the degree of SR but determines the time of its completion t_{compl}). For i_c below 500–700 A m^{-2}, the relation $t_{compl} \sim i_c^{1/2}$ is fairly well fulfilled, which implies that HSR kinetics in palladium are governed by the hydrogen delivery rate. The HSR rate at $i_c \geqslant 1000$ A m^{-2} is virtually independent of i_c. Relation (1) is equally well satisfied for the bulk of experimental data; for HSR, it is calculated that $V^* = (80-400) \times 10^{-24}$ cm^3.

It is worth noting when analyzing these results that the small value of V^* is in many cases much lower than V^* typical of SR processes driven by dislocation displacement [56–61]. For hydrogen-saturated samples at $\tau_0 \to \tau_s$, V^* tends toward the elementary volume V_0 (of roughly the same order of magnitude) corresponding to the hopping of a hydrogen atom as it diffuses into a crystal lattice. This fact is also regarded as indirect evidence that HSR kinetics are governed by the intensity of the hydrogen diffusion flow in the palladium crystal lattice. As a result, this process also determines the duration of the accumulation of hydrogen in the metal local microvolumes in concentrations sufficient for the formation of the β-phase.

X-ray studies showed that the onset of active microdeformation upon hydrogenation of palladium in the HDMA, HSR, and RMA regimes also coincides with the appearance of the first β-phase species in the near-surface layer. This circumstance relates large deformations of palladium undergoing hydrogen saturation to hydride formation (TPE) and the concomitant phenomena.

While heating Va metals and zirconium does not lead to the evacuation of hydrogen, it escapes palladium heated to a temperature much lower than the recrystallization temperature.

The full 'hydrogen saturation–heating' cycle in palladium after RMA is represented in Fig. 8. The high-rate deformation of a sample begins in the temperature range 150–250 °C (i.e., much lower than the recrystallization temperature $T_R \sim 350$ °C) in the direction opposite to its deformation during hydrogenation. The strain rate $\dot{\gamma}$ decreases significantly above 250 °C.

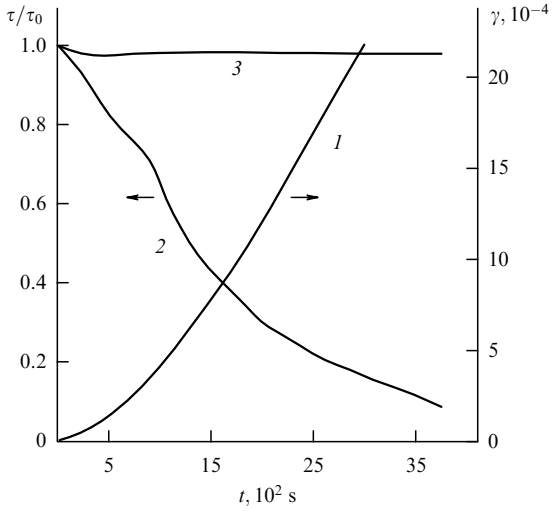

Figure 7. Creep strain at $\tau = 39$ MPa (*1*) and stress relaxation, $\tau_0 = 72$ MPa, (*2*) in the hydrogen saturation of palladium ($i_c = 500$ A m^{-2}). *3*, stress relaxation in the absence of saturation.

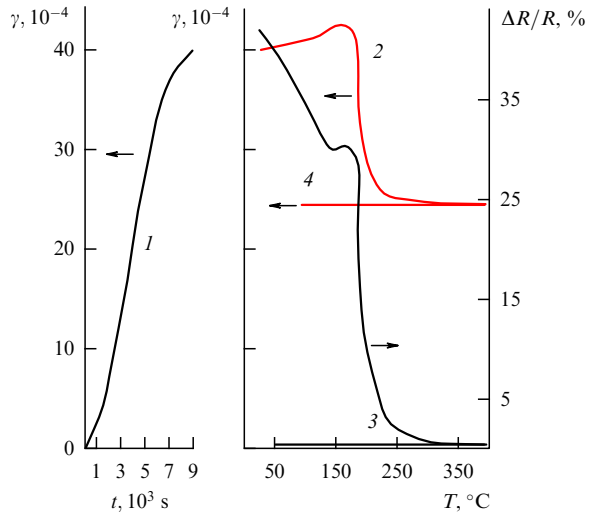

Figure 8. The effect of the duration of palladium saturation with hydrogen (*1*) at 300 K ($i_c = 1000$ A m^{-2}; $\gamma_t = 1.2$) and of subsequent heating (*2*) on the metal deformation and the variation of its electric resistance (*3*). *4*, palladium deformation upon cooling.

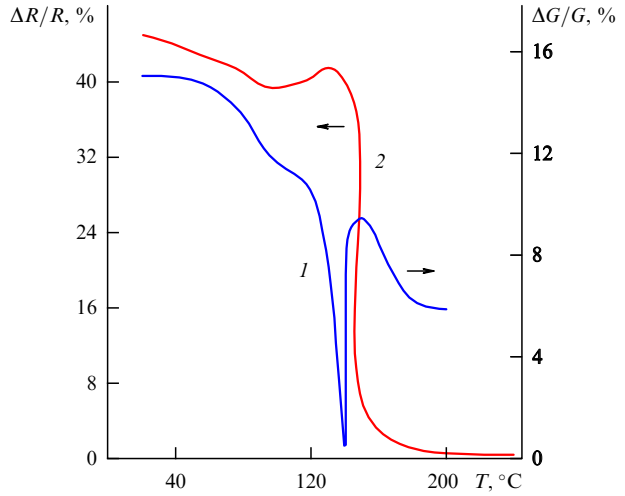

Figure 9. The effect of heating on the shear modulus (*1*) and electric resistance (*2*) of palladium preliminarily saturated with hydrogen ($i_c = 750$ A m^{-2}, $t = 7.2 \times 10^3$ s).

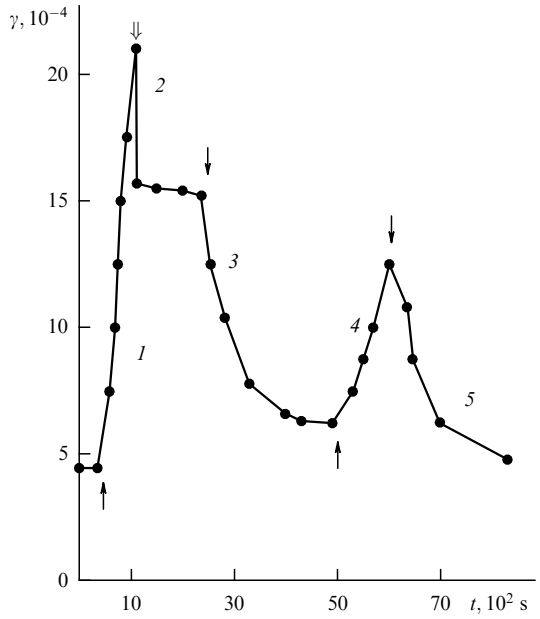

Figure 10. The concentration effects of the transformation plasticity and shape memory in hydrogen saturation (↑) and extraction (↓) in palladium. ⇓ indicates sample unloading ($i_c = i_a = 500$ A m^{-2}, $\tau = 12$ MPa).

Such deformations associated with heating hydrogen-saturated palladium are an order of magnitude (or more) greater than strains normally developing in this temperature range when heating affects an unsaturated plastically strained metal. Calculations indicate that the deformations are unrelated to dilatation effects inherent in hydrogen extraction from palladium.

One such self-evident mechanism of activation of the deformation response is the TPE strain [74, 78] in both forward ($\alpha \rightarrow \beta$) and backward ($\beta \rightarrow \alpha$) phase transformations. Repeated thermocycling in the temperature range of interest causes no additional deformation of palladium.

The dependence $\Delta R/R(T)$ shown in Fig. 8 (curve *3*) suggests a decrease in the electric resistance over the entire temperature range being considered. Two temperature ranges are distinguished on the $\Delta R/R(T)$ curve (25–150 °C and 200–250 °C) in which electric resistance changes at significantly different rates. A rapid decrease is observed in the same range where the most intense change of microdeformation occurs upon sample heating after RMA. It was shown that heating hydrogen-saturated palladium to 130–160 °C leads to a decrease in the hydride-phase lattice parameter ($a_\beta = 0.4039$ and 0.4026 nm before and after heating, respectively). Such a change in the lattice parameter is due to the partial escape of hydrogen from the metal. Heating to 200–250 °C results in the disappearance of any sign of the hydride phase on X-ray images and the recovery of the unit cell parameter characteristic of initial, hydrogen-unsaturated, palladium: $a_\alpha = 0.389$ nm.

Because the escape of hydrogen from palladium (under given experimental conditions) is an irreversible process, it is easy to understand why repeated thermocycling does not lead to a marked change in the electric resistance or a new manifestation of the after-effect.

Changes in the electric resistance and shear modulus in hydrogenated palladium samples at 120–200 °C, shown in Fig. 9, indicate that the plateau on the respective dependences corresponds to the condition of completion of the $\beta \rightarrow \alpha$ transition. Hydrogen begins to be actively released from the metal crystal lattice only at higher temperatures, when only the α-phase is present in the metal structure. This fact was not given proper attention by earlier authors.

The specific electrochemical properties of palladium (it does not dissolve in a sulfuric acid-based electrolyte in the anodic regime) were used to design unique experiments (Fig. 10) on hydrogen extraction from a Pd–H alloy in the anodic regime (with the sample as the anode).

The application of a positive potential to a loaded ($\tau < \tau_s$) sample results in no additional deformation (see Fig. 10). Changing the polarity (the sample as the cathode, hydrogen saturation regime) activates HDMA. If the sample unloaded at a certain saturation stage is again used as the anode (degasation), the deformation acquires the sign opposite to the one it had during saturation. The contribution of dilatation effects being small, the deformation at the degasation stage should be regarded as the concentrated SM strain. Indeed, extraction of hydrogen from the alloy leads to a decrease in the β-phase volume fraction and causes a well-apparent deformation. This process has all the external characteristics of the SM strain that develops in the active phase due to the realization of the concentration TPE. During the reverse phase transition induced by a decrease in the hydrogen concentration in the alloy, the strain accumulated at the preceding stage recovers. The recovery may be indirect evidence of the oriented character of β-phase precipitation during palladium hydrogenation in a stress field. The concentration effect of OTS is unobservable in this alloy.

The behavior of palladium during HS in the RMA regime is not only influenced by the preliminary annealing temperature but also depends on the magnitude of the preliminary torsional strain γ_t and alloying [26]. Alloying decreases RMA, although the hydrogen diffusion coefficient in Pd–Cu alloys exceeds that in pure palladium [106]. We note that RMA is fairly well apparent in palladium and iron but much less expressed in a Pd–Fe alloy [107, 108] than in either of its constituent metals. This difference is attributable to the influence of doping components contained in palladium on the characteristics of hydride incremental growth.

4. The isotopic effect in the deformation response of vanadium and palladium to saturation with hydrogen and deuterium

The isotopic effect of hydrogen in metals manifests itself in the structure of hydride and deuteride compounds, the general character and peculiarities of $M-H$ state diagrams, diffusion coefficients and their temperature dependence, solubility, superconductivity, electric and thermal transfer, electronic structure, etc. [13, 14, 109]. However, no research data on isotopic effects in the deformation response of metals and alloys have been available to date. This observation equally refers to the synergistic effects of accelerated microplastic deformation produced by the cooperative action of stress fields and high-intensity hydrogen or deuterium flows.

In vanadium, isotopic effects are clearly manifest in the values of the diffusion coefficient, characteristics of solubility and state diagrams. In palladium, isotopic effects in the diffusibility of hydrogen and deuterium atoms are less apparent. The solubility of deuterium and hydrogen in palladium is virtually identical; their state diagrams are also very similar [13, 14].

Figures 11 and 12 (see Refs [72, 110]) illustrate the isotopic effect in the deformation response of vanadium undergoing saturation with deuterium. The time before deformation, t^*, increases and its rate decreases compared with hydrogenation at the same cathode current density. As i_c increases, the values of t_D^* and t_H^* become closer to each other due to a superequilibrium concentrations of hydrogen (deuterium) in near-surface layers of the samples at large i_c. The hydrogen and deuterium diffusion coefficients in vanadium calculated for 300 K are $D_H = 5.21 \times 10^{-9}$ m^2 s^{-1} and $D_D = 2.1 \times 10^{-9}$ m^2 s^{-1}. These values reflect an explicit isotopic effect, although the relation $D_H/D_D = (m_H/m_D)^{1/2}$, where m_H and m_D are the respective isotope masses, is not usually fulfilled for metals with a BBC crystal lattice.

If the different deformation behaviors of vanadium during saturation with hydrogen and deuterium were due to the difference in the diffusion coefficients D_H and D_D alone, the relation $(D_H/D_D)^{1/2} \approx (t_H^*/t_D^*)^{-1/2}$ (where t_H^* and t_D^* are the times of the onset of active deformation under the effect of hydrogen and deuterium) would be satisfied. For 300 K,

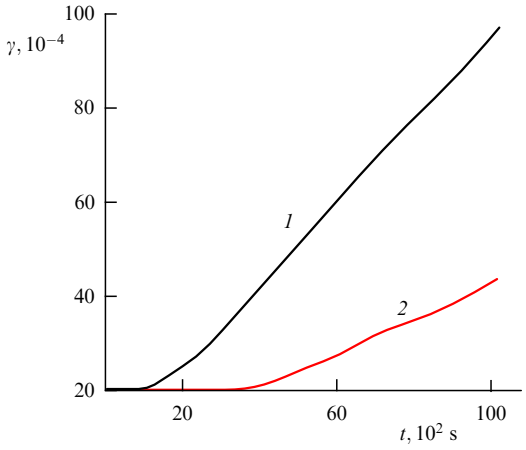

Figure 11. The effects of hydrogenation (*1*) and deuteration (*2*) on creep strain in vanadium ($i_c = 250$ A m^{-2}, $\tau = 98.4$ MPa).

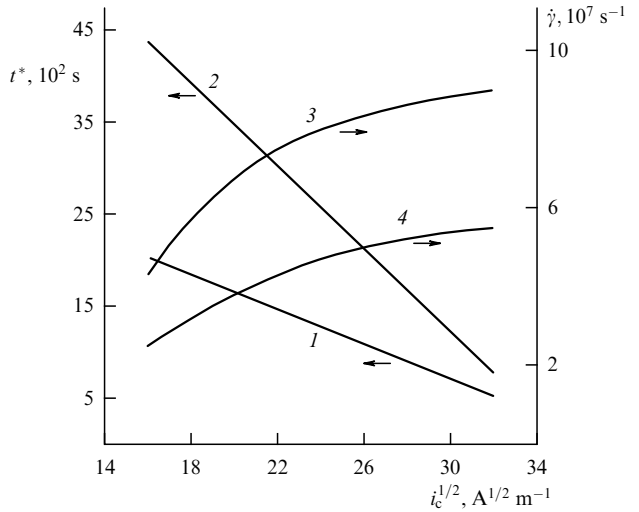

Figure 12. The effect of the cathode current density i_c on the time t^* of strain onset (*1*, *2*) and the strain rate (*3*, *4*) in hydrogenation (*1*, *3*) and deuteration (*2*, *4*) of vanadium.

$(D_H/D_D)^{1/2} = 1.57$. The ratio $(t_H^*/t_D^*)^{-1/2}$ is 1.43 for $i_c = 250$ A m^{-2}, 1.38 for $i_c = 500$ A m^{-2}, and 1.26 for $i_c = 1000$ A m^{-2}. Deviations for the calculated value are 10, 13, and 24%, respectively. In other words, differences between t_H^* and t_D^* tend to decrease with increasing i_c. This suggests an increase in the deviation from the quasiequilibrium conditions of hydrogenation and deuteration with the enhanced delivery rate of hydrogen isotopes into the metal.

Hydrogen solubility in metals is proportional to $i_c^{1/2}$ [51–53, 110]. Therefore, an increase in i_c accelerates the achievement of the hydrogen concentration in microvolumes of a metal needed for the formation of a hydride or a hydride-like cluster, i.e., for the activation of microplastic TPE. This implies fulfillment of the relation $(i_{c1}/i_{c2})^{-1/2} \approx t_{1H}^*/t_{2H}^*$. For hydrogenation with $i_c = 250$ A m^{-2} and $i_c = 500$ A m^{-2}, the ratio of respective times must be 1.41. Its real value 1.36 ± 0.03 is surprisingly close to the theoretical one. The same is true for deuteration, although the deviation from the calculated ratio is 15–20% at $i_c = 250$ A m^{-2} and $i_c = 500$ A m^{-2}. The smaller diffusion coefficient of deuterium appears to be responsible for the slowdown of diffusional pumping of its atoms from near-surface volumes; at lower current densities (surface oversaturation), the system passes from the quasiequilibrium to the equilibrium state. Broadly speaking, curves *1* and *2* in Fig. 11 are indicative of a linear relation between t_H^*, t_D^*, and $i_c^{-1/2}$, which confirms the validity of process regularities established in [26] for the given range of cathode current densities i_c.

Extrapolation of the relevant dependences up to the intersection with the axis of abscissas (see Fig. 12) suggests a certain i_c value at which $t_H^* \approx t_D^*$, meaning that critical concentrations of hydrogen isotopes needed for the emergence of a hydride or deuteride phase are reached within the same time period. In other words, the isotopic effect of hydrogen manifested in this form decreases as the rate of isotope introduction into a metal increases with the passage from quasiequilibrium to strictly nonequilibrium saturation conditions.

The qualitative similarity of the dependences $\gamma_H(t_H)$ and $\gamma_D(t_D)$, as well as the structural resemblance of isomorphic hydrides and deuterides, V_2H and V_2D, indicates that distortions arising during the oriented growth of deuteride

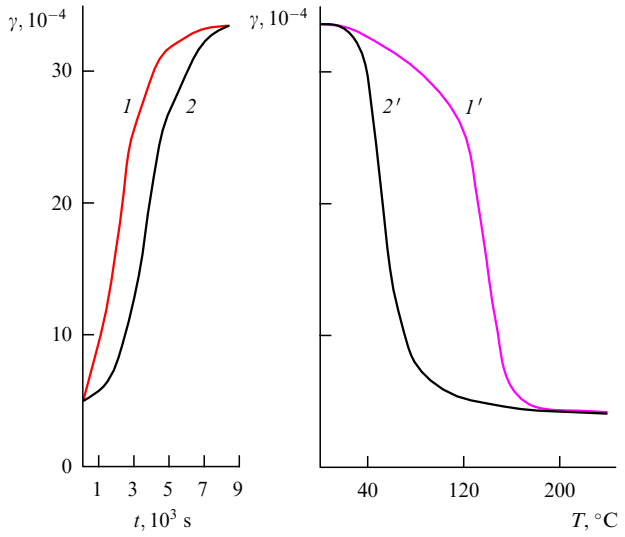

Figure 13. The effect of the duration of HS (*1*) and deuteration (*2*) on creep strain evolution ($i_c = 1000$ A m^{-2}, $\tau = 24.5$ MPa) and heat deformation ($\tau = 0$) in hydrogenated (*1′*) and deuterated (*2′*) palladium samples.

crystals and the growth coordinated with the stress field constitute the leading micromechanism of creep deformation accompanying deuteration. The oriented growth of hydrogen and deuterium-containing phases, coordinated with the stress state, is evidenced by the recovery (upon heating of preliminarily unloaded samples) of a substantial part of the deformation accumulated during hydrogenation or deuteration, which is the SM effect.

The calculated creep activation volumes at $\tau \to \tau_s$ are $V^*_H = (47 \pm 1) \times 10^{-24}$ cm^3 and $V^*_D = (40 \pm 5) \times 10^{-24}$ cm^3. Bearing in mind the practical errors, the strain characteristics determined in similar experiments can be considered virtually identical. The values of V^* thus obtained are much smaller than the ones inherent in dislocation creep mechanisms proper [87–92, 111–117].

Such small activation volumes, comparable with the volume of the elementary crystal lattice of vanadium, give evidence that in this case, the creep rate is controlled by the rate of hydrogen diffusion into the areas of hydride or deuteride crystal nucleation and growth.

A similar situation occurs in palladium undergoing the simultaneous effects of hydrogen isotope diffusion flows and stress fields (Fig. 13). Deuteration causes much weaker deformation than hydrogenation at the same cathode current density. The ratio $(t^*_D/t^*_H)^{1/2} = 1.47 \pm 0.05$ practically coincides with the square root of the isotopic mass ratio $(m_D/m_H)^{1/2} = 1.41$. Creep activation volumes at the initial stage of hydrogenation and deuteration are 91×10^{-24} cm^3 and 155×10^{-24} cm^3 ($1.5-2\,b^3$), respectively, and become practically identical at the most active saturation step (37×10^{-24} cm^3 and 40×10^{-24} cm^3).

Similarly to vanadium, hydrogenated and deuterated palladium develops an isotopic deformation response to heating (see Fig. 13), attributable to the reverse hydride or deuteride transformation. Lower temperatures of the onset and completion of the transition of deuterated samples to the α-phase are related to the so-called reverse isotope effect [13, 14, 108]: at equal concentrations and temperatures, the equilibrium pressure of deuterium in deuterides is higher than that of hydrogen in hydrides.

It can be concluded that differences in the diffusibility of hydrogen isotopes at 300 K, the structural specificity of newly precipitated phases, and the peculiarities of $M-H$ and $M-D$ state diagrams are the determining factors for deformation isotope effects.

5. Deformation effects in the hydrogen saturation of iron

The hydrogen diffusion coefficient in iron at 300 K is $(5-8) \times 10^{-11}$ m^2 s^{-1} [13, 14]. However, no hydride phases or hydride-like species have been found in iron under normal conditions, despite numerous attempts. A reduction in flow stress under the effect of electrolytic hydrogenation using the 'stiff' deformation scheme was first reported in iron undergoing tensile strain in excess of the yield point [36–50, 54]. Such studies are normally carried out at temperatures much below room temperature (150–200 K) using high-purity iron. In experiments close to 300 K, the decrease in the flow stress was insignificant (monocrystals) or absent (polycrystals).

Investigations into the synergistic deformation effects in iron of various degrees of purity and in its alloys were conducted with the use of a 'mild' load (torsion). Saturation of iron with hydrogen under loading below the macroscopic flow limit toward the HDMA regime (Fig. 14) significantly increased the deformation response [54–59, 118]. The onset of the active process was preceded by an incubation period t^*, whose length decreased with increasing the load or intensity of hydrogen delivery into the material. The following three most typical dependences $\gamma(t)$, corresponding to three loading paths, have been derived:

(a) once a maximum rate of the process is reached in the small stress range ($\tau < \tau_s$), the rate starts gradually decreasing;

(b) in the region of large plastic strains ($\tau \gg \tau_s$), continuous avalanche-like growth of a direct after-effect occurs. The process is highly irregular and is characterized by a stepwise strain variation in time;

(c) it ends in disintegration of the sample; under an intermediate stress ($\tau \approx \tau_s$), a gradual slowdown of the creep at a certain hydrogenation stage is followed by its acceleration and leads to metal degradation.

A diagrammatic view of research data (version 'a') in γ, ln t coordinates points to the possibility of representing the

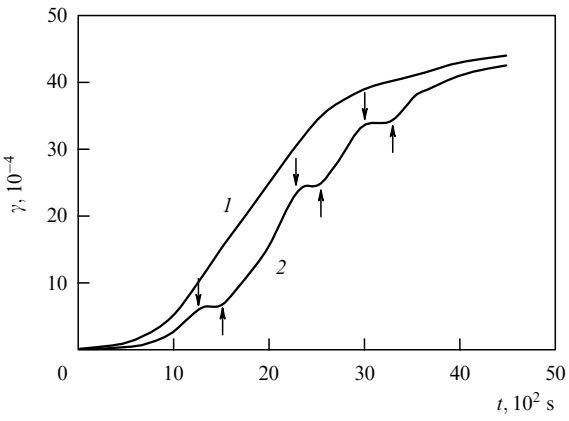

Figure 14. Creep in armco iron ($i_c = 1000$ A m^{-2}, $\tau = 180$ MPa): *1*, continuous hydrogenation; *2*, alternating switch on (↑)–switch off (↓) of the cathode current.

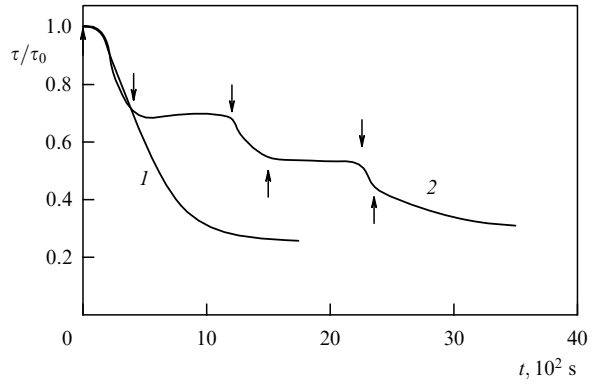

Figure 15. Stress relaxation in armco iron ($i_c = 1000$ A m^{-2}): *1*, continuous hydrogenation; *2*, alternating switch on (↑) – switch off (↓) of the cathode current.

bulk of experimental findings in the form of an approximating function of type (1). In the elastic strain range, the increase in τ is accompanied by a decrease in the volume V^*, which tends toward a certain constant value. Indeed, rough estimates of V^* are $V^* = (200-500) \times 10^{-24}$ cm^3 for small τ and $V^* = (30-50) \times 10^{-24}$ cm^3 for iron plastically strained in torsion. Of special interest is the similarity between the V^* values obtained from the analysis of HDMA data for iron and those calculated for the hydrogen-initiated deformation response in Va metals, zirconium, and palladium. Small V^* values close to the volume in which an elementary hydrogen diffusion act occurs suggest that the HDMA rate in this case depends on the hydrogen accumulation rate in the metal crystal lattice. The volume V^* increases at relatively small τ but is always much smaller than V^* for dislocation processes proper [112 – 119].

A specific feature of HSR kinetics in iron, distinguishing it from the 'classical' SR, is a nonmonotonic rate variation in time (Fig. 15), as in typical hydride-forming metals. Discontinuation of metal hydrogenation stops SR.

Representing the measured data in $\Delta\tau, \ln t$ coordinates ($\Delta\tau = \tau_0 - \tau$, where τ_0 is the stress at $t = 0$ and τ is the stress at a current instant $t > 0$) allows approximating the bulk of experimental findings with a set of straight lines ($\tau_0 = \text{const}$) corresponding to hydrogenation at different cathode current densities i_c. Therefore, as shown earlier for other hydride-forming metals, we can write

$$\Delta\tau = \alpha^* \ln(1 + \lambda t) .$$

The decrease in V^* as τ_0 increases is in excellent agreement with the well-known relation between these quantities and gives reason to regard this observation as more evidence in favor of the functional dependence $\Delta\tau(t)$ in the description of HSR (see also Ref. [120]).

The same exponential SR equations are equally suitable for the description of SR governed by dislocation mechanisms, the HSR in iron containing no stable hydride phase, and the HSR in typical hydride-forming metals (tantalum, niobium, vanadium). Therefore, SR equations of this type can be regarded as phenomenological equations unrelated to specific stress abatement mechanisms. The universality of such equations seems to reflect general consistent patterns of certain natural phenomena frequently described by exponential dependences.

Calculations show that for $\tau_0 < \tau_s$, $V^* = (250-500) \times 10^{-24}$ cm^3. These values are much smaller than V^* specific for the dislocation SR [112 – 118]. At the same time, V^* is significantly greater than the local volume V_H in which an elementary diffusion act takes place. In fact, for hydrogen diffusion in octahedral (or tetrahedral) pores of the iron crystal lattice at 20 °C, V_0 must not exceed $(30-40) \times 10^{-24}$ cm^3. This value is close to V^* for HSR in iron plastically strained in torsion. As $\tau_0 \to \tau_s$, $V^* \to V_0$ and for $\tau_0 > \tau_s$, V^* is virtually independent of the degree of metal plastic strain. Therefore, both the rate and the magnitude of HSR are determined on the one hand by the metal structure and on the other hand by the hydrogenation conditions and hydrogen diffusion characteristics in a given material. Extrapolation of the straight lines describing HSR in the $\Delta\tau, \ln t$ coordinates to the time axis gives sections whose size depends on both i_c and τ_0. From the physical standpoint, this fact can be interpreted as the existence of a certain preliminary period t^* preceding the active stage of HSR. The length of this period is inversely related to the degree of metal saturation with hydrogen (below i_c). The presence of the preparatory period t^* manifests itself in peculiar features of HSR kinetics that distinguish it from the classical SR.

If t^* is supposed to be the time necessary for attaining the desirable hydrogen concentration in a certain local volume of a metal, then the inverse proportion between t^* and $i_c^{1/2}$ can be expected in the general case; this assumption is confirmed experimentally. All the curves converge at a single pole i_c^*, which means that the functional relation between the length of the preparatory period, the cathode current density, and the applied stress value can be described by Eqn (2):

$$\ln t^* = \text{const}\,(i_c^*)^{-1/2} \tau_0^{-1} \left(\sqrt{\frac{i_c^*}{i_c}} - 1 \right) .$$

Thus, the deformation response in iron is described by the same empirical relations as HSR in hydrogen saturation of typical hydride-forming metals (vanadium, tantalum, niobium, and palladium).

The hydrogenation of iron plastically strained in torsion results in an increase (by one or two orders of magnitude) in the rate and the magnitude γ of the reverse mechanical after-effect [54]. Discontinuation of hydrogenation causes a sharp slowdown of the deformation response. Reswitching the polarization current in all cases induces a new increase in γ in time ($\Delta\gamma$); however, the cumulative mechanical after-effect in the case of intermittent hydrogenation usually approaches but always remains somewhat smaller than the γ characteristic of a continuous delivery of hydrogen. A relative change in deformation caused by the introduction of hydrogen into α-Fe is significantly greater than effects observed in earlier studies of tensile strains in iron of varying degrees of purity [36 – 51].

It was shown that the reverse mechanical after-effect along a constant gradient over the sample cross section is unrelated to the sample diameter within the examined range of its variations. This means that a constant strain gradient rather than γ_t needs to be maintained in order to obtain comparable responses from samples of different diameters. This fact clarifies the role of the scaling factor in the oversaturation of metals with hydrogen.

In annealed Fe – C alloys having a two-phase ferrite – perlite structure, the increment of the microscopic elastic after-effect (MEA) during HS is much smaller than in pure

iron. RMA effects in martensitic steels and in Fe + 3% (weight) Si are relatively low. Experiments with austenitic steels also fail to reveal a noticeable enhancement of the reverse mechanical after-effect even in HS with a high cathode current density ($i_c > 5000$ A m^{-2}). In other words, acceleration of the microplastic deformation as a result of HS should be expected only in iron-based alloys with a high ferrite content and a large hydrogen diffusion coefficient. This explains why neither a decrease nor an increase in the flow stress in aluminium and austenitic steel was observed in the HS experiments in Refs [121 – 123].

To understand the problem better, experiments were conducted on alloys of iron with nickel, aluminium, manganese, chromium, and silicon, each containing 2% of the doping element (by weight). The basic metal was carbonyl iron (0.0046% C). The alloying of iron was undertaken with the object of manufacturing alloys with modified characteristics (first and foremost, diffusion properties) while retaining the single-phase ferrite structure [124 – 132]. It was shown that the introduction of doping elements forming substitution solid solutions with iron slightly changes the form of the $\gamma(t)$ dependence and decreases the MEA upon hydrogenation of the alloy. The reduction is especially noticeable when iron is doped with silicon and less so for nickel and aluminum. One result of the introduction of doping elements into the crystal lattice of iron is the altered mobility and solubility of hydrogen in the alloy structure. More importantly, such alloying decreases the effective hydrogen diffusion coefficient (D_H) in the metal [6, 127 – 132]. This effect has a dual nature. On the one hand, the electron properties of the doping element correlate with hydrogen diffusion in the alloy [130]. On the other hand, doping elements modulate the energetic properties of the traps and can themselves capture hydrogen. It turned out that doping elements with weak metallic properties have the strongest influence on D_H and are responsible for the greater reduction in the MEA upon hydrogenation of the alloy, which implies that when all other conditions are equal, the major influence of doping on the MEA in the case of RMA primarily manifests itself in the change in the effective hydrogen diffusion coefficient in iron-based alloys. This inference agrees with earlier conclusions regarding the role of hydrogen diffusion characteristics in the enhancement of MEA upon hydrogenation. If this conjecture is correct, there are good prospects for the rapid assessment [133] of the influence of doping elements on hydrogen diffusion properties in iron from the synergistic effects of the deformation response.

The reported experiments with iron showed that the activation effect of HS under different loading conditions is manifested, as in other hydride-forming metals, in the reverse mechanical after-effect, stress relaxation, and creep. The importance of information on the behavior of iron-based alloys during loading and HS was demonstrated in applied studies [134, 135].

Concluding this section, we consider it appropriate to dwell on a few topics related to investigations into the hydrogen interaction with dislocations, the dislocation paradigm, and its applicability to the explanation of synergistic effects in iron and other metals and alloys. A great number of research papers and reviews have appeared in the literature devoted to the interaction of hydrogen with metals and alloys. Of special interest, in the context of the synergistic effects of microplasticity, are papers where methods are proposed for controlling deformation processes and reducing flow stress. Of the greatest value are the theories concerned with direct interactions between hydrogen and dislocations.

The greatest attention should be given to experiments on internal friction (IF). We emphasize two facts in this connection. The condensation temperature of a hydrogen atmosphere is found not from the Boltzmann distribution generally accepted for Cottrell atmospheres of nitrogen, oxygen, or carbon atoms but from the Fermi – Dirac distribution [136]

$$\frac{c}{1-c} = \frac{c_0}{1-c_0} \exp \frac{U_b}{kT}, \tag{4}$$

where c is the hydrogen concentration at a dislocation, c_0 is the mean hydrogen concentration in a metal, and U_b is the energy of hydrogen bonding with the dislocation. Different authors estimate the condensation temperature as being below 200 K.

The peaks of IF for hydrogen have been measured in the temperature range 40 – 170 K; they were absent at higher temperatures. The possibility of increasing the dislocation density by hydrogen diffusion flows has also been discussed.

The most consistent theory was proposed in Refs [137, 138], where it was suggested that joint action of a stress field and HS may significantly increase the dislocation density. According to these papers, the elastic energy of dislocations can be lowered by segregating hydrogen atoms from U_d to U_d^*. Then the external stress needed for a Frank – Reed source to operate can be represented as

$$\tau_0 = \frac{U_d}{Lb} \quad \text{and} \quad \tau_0^* = \frac{U_d^*}{Lb}, \tag{5}$$

where L is the length of a dislocation segment and b is the Burgers vector. Hence, there is a possibility of activating the dislocation source.

Furthermore, elastic interactions of hydrogen and dislocations are considered in this theory under the assumption that hydrogen atoms cause strong tetragonal distortions (in disagreement with the results of IF measurements and other studies). Postulating tetragonal distortions permits the authors to suggest the existence of an asymmetric hydrogen atmosphere around the dislocations. The energy U of interaction between a screw dislocation and its hydrogen atmosphere is

$$U = \int \rho_U \, dV, \tag{6}$$

where ρ_U is the interaction energy per unit volume.

Expanding U with respect to directions x and y yields an additional force acting on the screw dislocation. The defining relation for 200 K and the mobile dislocation density 10^{10} m^{-2} is written as

$$\frac{V_H}{V_d} = 8 \times 10^{-2} \frac{1}{T\dot{\varepsilon}} \exp\left(-\frac{828}{T}\right), \tag{7}$$

where V_H and V_d are the respective dislocation speeds with the hydrogen atmosphere and without it and $\dot{\varepsilon}$ is the strain rate.

Relation (7) indicates that an increase in $\dot{\varepsilon}$ at standard temperatures causes the ratio V_H/V_d to decrease. If $V_H/V_d < 1$, no asymmetric hydrogen atmosphere is formed.

In other words, hydrogen must not decrease the effective flow limit in samples undergoing a very high-rate deformation.

The values of V_H/V_d vary with temperature in the same way as with $\dot{\varepsilon}$. This implies the existence of a critical temperature T_{cr} at which the hydrogen diffusion rate equals the dislocation movement rate. For example, T_{cr} is approximately equal to 130 K for $\dot{\varepsilon} = 10^{-2}$ s^{-1} and 240 K for $\dot{\varepsilon} = 10^{-1}$ s^{-1}. The critical temperature T_{cr} decreases as $\dot{\varepsilon}$ increases. If the test temperature is higher than T_{cr}, the asymmetric hydrogen atmosphere surrounding a screw dislocation generates an additional force that affects it and thereby lowers the effective flow limit. When $T \gg T_{cr}$, the additional force τ_H decreases and τ_c increases.

On the other hand, when the temperature is very low, $V_H > V_d$, a braking force slows down dislocation movement.

At approximately the same time, an entirely new mechanism of hydrogen action on the plastic behavior of metals was proposed in Refs [139, 140]. It was assumed there, first, that the chemical driving force may transform into a mechanical effect of dislocation movements in the course of hydrogen introduction or removal. Such a transformation is feasible if the hydrogen diffusion along a dislocation is faster than the lattice diffusion; in this case, dissolution or evacuation of hydrogen facilitates dislocation movements. Second, the high fugacity (volatility) of hydrogen already suffices to enable it to overcome the dislocation nucleation barrier and activate many surface sources of dislocations. Also, it is conducive to the appearance of new dislocations that may stimulate penetration of hydrogen into the sample.

The chemical driving force acting on the dislocation line along which hydrogen diffuses with a volatility f_0 and from which hydrogen with a volatility f penetrates into the crystal lattice is represented for shear stresses as

$$\tau = \frac{nkT}{2} \ln \frac{f_0}{f}\,, \tag{8}$$

where n is the number of hydrogen atoms leaving the dislocation unit length when dislocations travel over a distance equivalent to the Burgers vector b, k is the Boltzmann constant, and T is the temperature. For example, at $f_0/f = 2$ and $n = 10^{10}$ hydrogen atoms/mol, the chemical driving force is equivalent to the shear stress of 306 MPa at 200 K. These values are usually sufficient for dislocation movements to begin. The effect may be lower if the temperature increases and n decreases faster than kT in Eqn (8) increases. On the other hand, a decrease in temperature may reduce the effect due to a decrease in kT and saturation of the dislocation nucleus with hydrogen.

We note that the volatility f must be higher than in the crystal volume. The degree of excess depends on the hydrogen desorption rate from dislocations into the crystal lattice, the dislocation movement rate, and the tubular diffusion rate along dislocations.

Equation (8) can be used to estimate equivalent stresses necessary to activate surface sources of dislocations if f_0 is the volatility of hydrogen introduced through the surface and f is the volatility after the hydrogen capture by dislocations coming from the surface. The volatility ratio $f_0/f = 1000$ is equivalent to the application of shear stresses about 3 GPa; this is sufficient for the activation of many surface dislocation sources. Evidently, the volatility ratio for dislocation sources at grain boundaries should be smaller.

The authors believe that this mechanism explains the following effects of hydrogen on the plastic behavior of iron and steel:

- a decrease in the flow stress and an increase in the creep rate or the SR rate;
- strengthening upon hydrogenation due to an increased dislocation density.

We consider the possibility of applying concepts of hydrogen-dislocation interactions to the explanation of RMA in iron.

It appears appropriate to speak of enhanced dislocation mobility due to the reduction of the Peierls barrier height by hydrogen [141 – 143] only in application to high-purity iron at relatively low temperatures, at least below 300 K. The author of Ref. [144] does not exclude the possibility that hydrogen may increase Peierls – Nabarro forces in iron. RMA studies have shown that the purity of iron (comparing the responses of armco iron, carbonyl iron, and zone-purified iron to hydrogenation) is inessential. Moreover, the influence of the Peierls relief must decrease with increasing the dislocation density, i.e., with increasing γ_t, due to stronger interactions between dislocations. However, RMA experiments have not confirmed such a relation between γ_{op} and γ_t.

For the same reason, an increase in the dislocation density [145] by a hydrogen diffusion flow cannot serve as an acceptable RMA mechanism (this assumption contains an analogy with the so-called 'electroplastic effect') [146 – 148]. An argument in favor of this inference was derived from experiments on the influence of the aging of samples with torsional strain on RMA in iron. No apparent decrease in MEA was documented despite the markedly restricted mobility of dislocations in metals due to strain aging. Moreover, internal stresses caused by plastic strain simultaneously underwent relaxation. Taken together, these observations questioned the hypothesis of the linear stretch of dislocations under the effect of hydrogen.

The notion of softening due to hydrogen-driven bending of screw dislocations is widely used to explain the effects of dynamic hydrogenation at temperatures much below room temperature [48, 149], whereas acceleration of the RMA microdeformation occurs at room temperature. First, we note that in dynamic hydrogenation under torsional strain, the decrease in the flow tension in the optimal temperature range is especially pronounced in high-purity metals and in samples of a monocrystalline structure. RMAs in torsion are practically unknown. Second, in Refs [46 – 50], the reduction of flow stress was always preceded by a certain degree of plastic strain; this means that the authors observed the interaction of hydrogen with 'fresh' dislocations. In those experiments, the oversaturation with hydrogen appears to have been insufficient for independent activation of dislocation sources.

The results of electron microscopic studies [47, 150, 151] appear to confirm the hypothesis of electron-assisted movements of screw dislocations and decreased stress at the start of dislocation source activation. However, it should be borne in mind that the behavior of a thin foil is hardly equivalent to that of a bulk specimen. Moreover, conditions of electrolytic hydrogenation and hydrogenation in the gas phase in the electron microscope column are essentially different. Finally, electron microscopy produces virtually similar images of hydrogenated nickel [152, 153] and iron [47, 150, 151] foils, while RMA experiments with nickel fail to demonstrate accelerated microdeformation.

The hypothesis of additional stress conditioned by asymmetry of the hydrogen atmosphere surrounding and acting on screw dislocations [137, 138] is equally inapplicable as such to the description of the results of RMA experiments.

This inference ensues, for instance, from a purely formal analysis of Eqn (7) at $\dot{\varepsilon} = 0$ and $V_d = 0$ corresponding to the instant of hydrogen introduction into a metal in RMA experiments. This relation loses physical meaning when the applied stresses do not cause active deformation. At the same time, the hydrogen concentration in iron of the order of 10^{-5} at 300 K is readily attainable in electrolytic hydrogenation. According to [140], this concentration must lead to a reduction of stress by more than 50%. But in the majority of studies, the flow stress in both preliminarily hydrogenated samples and specimens hydrogenated when being stretched does not decrease but, on the contrary, increases compared with untreated samples. Moreover, other metals having a BBC lattice (V, Nb, Ta) show no appreciable acceleration of RMA when the hydrogen concentration in the solid solution is significantly higher than in iron. It is difficult to explain the effects of alloying, strain aging, cathode current density, and torsional strain on MEA in terms of the hypothesis in [138].

We emphasize that most of the above approaches are equally applicable to the description of phenomena arising from loading preliminarily hydrogenated metals and metals undergoing dynamic hydrogenation. They ignore the nonequilibrium character of processes proceeding in a metal undergoing concurrent hydrogenation and deformation.

The hypothesis in [139, 140] is essentially free from this drawback and, more than others, applicable to the analysis of metal behavior in real experiments on dynamic hydrogenation, because the existence of a diffusion flow in the sample is an indispensable condition for realization of the model. Naturally, saturation with hydrogen first and foremost activates dislocation sources in the surface layers of the sample. Therefore, RMA must depend on the surface-to-volume ratio characterizing the sample. However, no such dependence was documented in the above studies.

To conclude, the dislocation paradigm explains neither synergistic effects in iron and iron-based samples nor even results obtained in the framework of the 'stiff' loading diagram. The discussion of qualitative, let alone quantitative, agreement between theory and experiment is not in question at all. Also important is the fact that these theories are designed to interpret experimental data obtained at 200–170 K, whereas synergistic effects of microplasticity actively develop at 300 K. With the stiff mode of loading, a reduction in the flow stress related to hydrogenation is usually absent. Also, it is understandable that the dislocation paradigm cannot explain the patterns of behavior and synergistic effects in typical hydride-forming metals and other alloys interacting with hydrogen.

6. The deformation response and change of properties in hydrogen-saturated shape-memory alloys

The available experimental data [64, 68, 154, 155] indicate that the influence of hydrogen on the deformation response becomes especially well apparent as the system approaches the concentration or temperature phase transition point. In this context, TiNi-based alloys (nitinols) are of great interest; they undergo thermoelastic-type martensitic transformations and exhibit the full spectrum of strain effects, viz. TPE, OTS, and SM effects. Moreover, depending on the alloy composition, the temperature of martensitic transformations may be higher or lower than room temperature, at which electrolytic hydrogenation is usually performed. Deviation of the phase transition temperature from the hydrogen saturation temperature creates a unique opportunity for the assessment of the role of premartensitic instability of the crystal lattice in hydrogen interactions with such alloys.

Nitinol alloy (see, e.g., Refs [156, 157]) is a chemical composition of two hydride-forming components. The crystalline structure of the initial high-temperature phase (β-phase) of TiNi corresponds to a B2-type atomically ordered crystal lattice with the unit cell parameter $a = 0.3015$ nm. An unambiguous definition of martensite crystalline structure is lacking. Different authors describe it either as monoclinic (of two types): $a = 0.519$ nm, $b = 0.496$ nm, $c = 0.425$ nm, $\gamma = 99°$; $a' = 0.519$ nm, $b' = 0.552$ nm, $c' = 0.425$ nm, $\gamma' = 116°$ or as monoclinically distorted B19′orthorhombic ($a = 0.2889$ nm, $b = 0.412$ nm, $c = 0.4622$ nm, $\varphi = 96.8°$), etc. [156–159].

It is shown in Refs [160, 161] that the hydrogen absorption by the high-temperature phase (B2) at 300 K is approximately 2.5 times the absorption by the martensitic phase (B19′). The amount of absorbed hydrogen varies depending on structural changes in the course of thermal treatment. However, no absorbed hydrogen is removed from the alloy upon thermocycling close to the martensitic transformation (MT) point. At temperatures between 770 and 1170 K and the pressure 1.3×10^5 Pa, hydrogen in the B2 phase dissolves exothermally [162] and forms an interstitial solid solution. The hydrogen solubility obeys the Sieverts law and, in TiNi alloys, is described by the Arrhenius law. Extrapolation to 300 K gives $D \sim 4 \times 10^{-9}$ m^2 s^{-1}; this value is roughly of the same order of magnitude as the highest known hydrogen diffusion coefficient in metals: 2×10^{-9} m^2 s^{-1} (vanadium). The hydrogen diffusion coefficient directly measured in an equiatomic TiNi alloy at 300 K [63] is 6.45×10^{-9} m^2 s^{-1}.

The influence of hydrogen on the thermoelastic MT is attributed to its action on the stability of the B2-phase crystal lattice [163–169]. X-ray analysis revealed a significant decrease in the characteristic temperature and an increase in mean-square dynamic atomic displacements in HS of stress-tolerant and intolerant TiNi alloys. Reduction of these values is as significant as the B2 → R phase transition temperature to the loss of stability of the β-phase crystal lattice. It is concluded based on these data that hydrogen reduces the stability of the B2-phase crystal lattice and thereby creates necessary conditions for the induction of a thermoelastic MT, even in alloys that do not undergo such transformations at temperatures down to −196 °C.

Investigations of the synergistic effects of the MT showed that the introduction of hydrogen at 20 °C into nitinols with different temperatures of the onset of the martensitic transformation initiates and multiply accelerates creep strain (Fig. 16), causes dilatation, and increases the electric resistance and shear modulus [170, 171]. Hydrogenation of TiNi alloys initiates an anhysteretic B2 → R transition. Single HS ensures long-term (for many years) retention of alterations in the sequence of structural-phase transformations in these alloys upon thermocycling. The influence of hydrogen on titanium nickelide cannot be totally eliminated, even by heating of the alloy to 800–900 °C. The hydrogen-induced TPE and SM effects observed in these studies are essentially different from the known strain effects of HS in

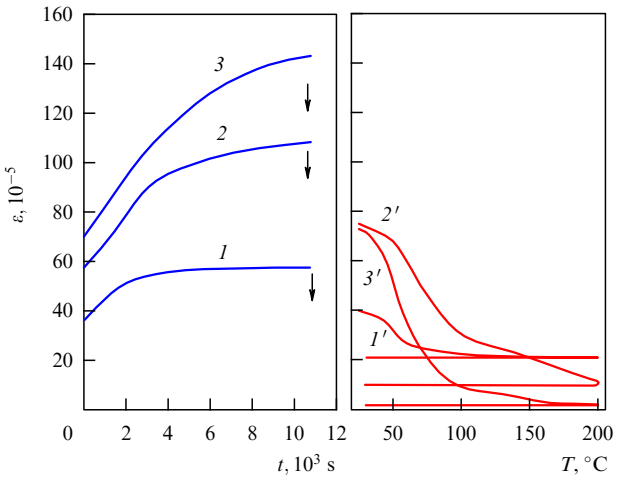

Figure 16. The effect of HS duration (*1*–*3*) and subsequent thermocycling (*1′*–*3′*) on deformation of a TiNiFe alloy: *1*, $\tau = 35$ MPa; *2*, $\tau = 70$ MPa; *3*, $\tau = 105$ MPa. ↓ indicates unloading.

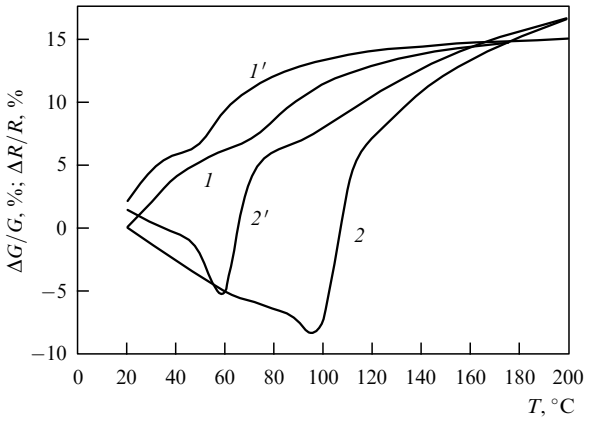

Figure 17. The effect of the thermocycling of a TiNiFe alloy on electric resistance (*1*, *1′*) and shear modulus (*2*, *2′*): *1* and *2*, heating; *1′* and *2′*, cooling.

metals of the Va subgroup. Hydrogen changes the PT sequence or intensity during HS of two-phase TiNi-based alloys as a result of additional loss of resistance of the alloy's crystal lattice to shear strain. As shown by the analysis of experimental data, this effect is responsible for the opening of new phase transformation channels without alteration of the general type of martensitic transformations intrinsic in a given alloy.

The totality of the available data indicates, at variance with what was previously thought, that hydrogen interactions with TiNi intermetallide do not reduce to the trivial effect of hydrogen absorption on the structure of the material and are unrelated to the emergence of hydride phases or 'hydrogen' martensite [165–168].

Phase transformations in nitinol alloys upon cooling from the homogeneous B2-phase region are preceded by a well-apparent temperature interval of shear modulus reduction (Fig. 17). This reduction also occurs in a diffusion-cooperative PT and in HS or thermocycling of certain hydride-forming metals and M–H alloys [74]. This means that the reduction of the shear modulus when the temperature approaches that of the thermoelastic martensitic or diffusion-cooperative PT is a universal feature of such phase transformations. This effect is underlain by a decreased resistance of the alloy's crystal lattice to shear strains ('softening' of the shear modulus).

Experiments on the synergistic effects of microplasticity in hydrogen interactions with certain transition metals showed that superequilibrium concentrations of hydrogen also contribute to the reduction of the resistance of the alloy to shear stress (degradation of the shear modulus). This effect of hydrogen becomes stronger as the structural state of the alloy comes closer to the transition to a new phase modification in advance of diffusion-cooperative phase transformations or in thermoelastic martensitic transformations in nitinol-like alloys, suggesting an amorphizing effect of hydrogen in metal alloys.

Of special interest for the analysis of the role of the structural state of metals and alloys in manifestations of HS-induced microplasticity are the results of research on microdeformation in hydrogenated amorphous metal alloys (AMAs) intrinsically devoid of a long-range order in the atom arrangement.

7. The deformation behavior of amorphous metal alloys interacting with hydrogen

Despite many uncertainties, the principal mechanisms of the hydrogen interaction with AMAs are currently rather well known. AMAs are known to absorb 40–50% more hydrogen than crystalline alloys [172–174]. They retain the roentgen-amorphous state after HS. Hydrogen absorption increases the width of the halo and causes its displacement toward smaller reflection angles; this suggests an increase in interatomic distances. The hydrogenation of AMAs leads to an increase in the electric resistance [174], a decrease in the superconducting transition temperature, and an increase in the Curie temperature [175]. The hydrogen diffusion coefficient in AMAs is higher than in their crystalline analogs [176], but the two diffusion mechanisms are believed to be different. The hydrogen interaction with defects in AMAs was shown to obey the Fermi–Dirac statistics [177]. Hydrogen is supposed to occupy a variety of atomic positions in metal glasses [172]. Similarly to crystalline alloys, AMAs undergo embrittlement under the action of hydrogen [172, 176, 178], although it does not always result in complete brittle fracture.

All previous studies suggest that a necessary condition for the manifestation of mechanical instability is a superequilibrium concentration of hydrogen in the bulk or in local volumes of the material. This condition is satisfied in the case of a high hydrogen diffusion coefficient in a metal or an alloy at the HS temperature. AMAs satisfy these requirements.

Studies of deformation response in iron- and cobalt-based AMAs to simultaneous loading and HS [179–181] have shown that the introduction of hydrogen initiates creep strain that continues until sample disintegration (Fig. 18). Its rate varies as it does in crystalline alloys undergoing hydrogenation. X-ray studies have not revealed the formation of new crystalline structures or the emergence of a crystal hydride phase.

Creep acceleration and an increase in the electric resistance in the course of HS were observed in another well-known alloy, $Pd_{77.5}Cu_6Si_{16.5}$.

Thus, hydrogen initiates creep in a variety of AMAs loaded much below the elastic strength. It is essential that this strain develops only in the case of active pumping of

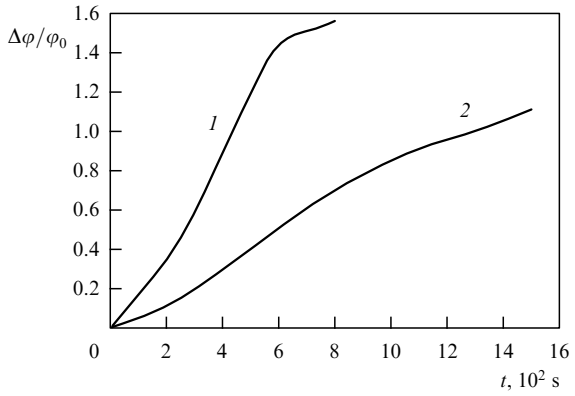

Figure 18. The effect of HS duration on the AMA ($Ni_{60}Nb_{40}$) deformation in torsion: *1*, $M_t = 40 \times 10^{-6}$ kG m, $i_c = 100$ A m^{-2}; *2*, $M_t = 40 \times 10^{-6}$ kG m, $i_c = 20$ A m^{-2} (M_t is the torque).

hydrogen into an AMA. Termination of its delivery ($i_c = 0$) immediately stops further progress of the strain. This means that this phenomenon occurs only under the joint action of two factors, the stress field and the high-intensity hydrogen diffusion flow.

Torque loading of AMAs leads to relatively stronger deformation effects than tensile strain. This is a common feature in the HS of crystalline materials in a stress field, probably occurring because the most pronounced synergistic effects of this type manifest themselves in the presence of a high-gradient force and concentration fields. Stretching induces a more homogeneous stress state and hence a lower strain. On the other hand, torsional strain produces a 'milder' load, which offers a relatively larger margin of plasticity than tensile strain.

A known approach to examining SR in AMAs [182] is the annealing of an alloy strip bent on benders of different radii with the subsequent determination of the strip curvature radius. But the application of this method to the study of SR in an AMA undergoing HS encounters difficulties arising from the loss of the strip shape after HS; the hydrogenated strip shows practically no shear resistance for some time after HS. The reaction of this material to an external force impact compares with the reaction of a tissue strip (resistance to tensile stress and lack of shear strength). This makes measurement of the curvature radius of a strip taken off the bender impracticable.

In experiments with a single-sided support of an AMA sample, the measured parameter was the ratio d of the deviation X of the loose end of the sample to its initial length L. The carrying capacity of the fixed AMA sample (Finemet alloy, $Fe_{78}Nb_{3.5}Cu_1B_4Si_{13.5}$) was practically lost during its electrolytic hydrogenation [183–188] (Fig. 19). But the shape of the sample was restored after HS during a two-stage process. At the first stage, the shear strength recovered, and the formless sample again acquired the characteristic shape of a metal strip. At the second stage, the sample returned to the 'initial' (horizontal) position.

Similar results were obtained with other AMAs, e.g., $Fe_{81}B_{14}Si_5$, $Fe_{65}Co_{20}Si_5B_{10}$, and $Fe_5Co_{70}Si_{15}B_{10}$.

Cobalt-based AMAs are subject to a smaller strain upon HS than iron-based alloys and require more time to restore the original shape than $Fe_{81}B_{14}Si_5$ and Finemet. If samples held long enough to recover the initial shape are again saturated with hydrogen following the previous schedule,

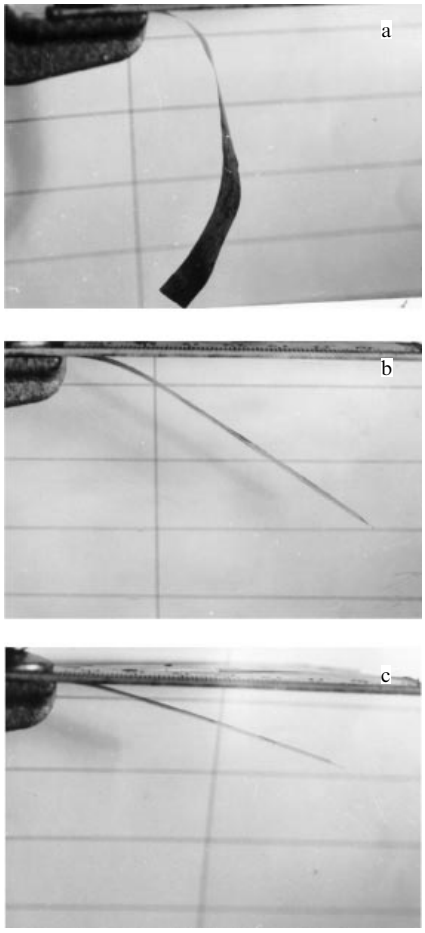

Figure 19. An amorphous strip of a Finemet alloy immediately after HS (a), 2 h after HS (b), and 10 h after HS (c).

they show virtually the same behavior as in the first HS, but shape changes and concomitant phenomena are less expressed.

Thus, the necessary condition for a reversible loss of shape (RLS) is HS of iron-based AMAs at superequilibrium hydrogen concentrations at the surface of the sample and inside it. In this case, the macroscale behavior of AMA resembles the behavior of amorphous materials under their own weight (non-Newtonian flow).

The RLS is not an SR in the traditional sense. A true relaxation process, *regardless of its mechanism*, is characterized by the transition of elastic to plastic strain conditioned by an irreversible change of the sample shape. This phenomenon is not observed in RLS experiments. It gives reason to believe (see, e.g., Ref. [188]) that hydrogenation of AMAs causes dramatic structural reorganization in the treated material. For the purpose of this review, the AMA structure is understood as a certain averaged spatial (short-range order) atom arrangement chemically and topologically characteristic of a specific alloy.

The above inference is based on the results of experiments designed to assess the dependence of RLS on the AMA annealing temperature prior to HS. In a range of annealing temperatures below 200 °C, HS had practically no effect on d. Heating Finemet to 300 °C and holding it at this temperature for 30 min markedly diminished RLS. As shown in Refs [182, 188], this is the temperature at which a structural reorganization (structural relaxation) in the majority of iron-based

AMAs begins. This accounts for the alteration of many physical properties, e.g., the Barkhausen noise power spectrum [189 – 192]. Annealing of alloys at higher temperatures gives rise to a new structural state different from the original one. This may be supposed to account for the virtually total disappearance of the RLS effect after annealing at $T \geqslant 400\,^{\circ}\mathrm{C}$.

These results indicate that the deformation response of AMAs being saturated with hydrogen is a highly sensitive indicator of their susceptibility to variations in the structural state of alloys.

It turns out that shape restoration is a high-speed thermal process activated by heating to 200 °C. We note that neither our nor other authors' studies in the above temperature range revealed structural relaxation in iron-based AMAs.

The activation energy of shape restoration for Finemet was found to be 0.4 ± 0.1 eV and the characteristic time $\sim 10^{-2}$ s. This energy value is at variance with 0.38 eV reported in Refs [193 – 195], but the hydrogen-induced reorganization of an AMA containing no iron was considered there; the characteristic time was estimated as 6×10^{-14} s [193, 195]. This value is comparable with the duration of an elementary hopping of a hydrogen atom during diffusion in the metal crystal lattice. But in the present case, it is much larger than that, indicating that the shape relaxation process involves collective rather than single displacements of atoms from their initial positions.

The following note is in order to summarize the results of research on the nature of reversible loss of shape. Hydrogen, along with ten other elements (C, H, N, B, Be, O, F, S, P, and Si), is the most efficient amorphizer [196]. At 1 atm%, it has the same amorphizing effect on metals as other amorphizing additives at ~ 15 atm%. However, the solubility of hydrogen being low, its overall action is not as conspicuous as when it saturates metals under near-equilibrium conditions.

The situation changes dramatically when hydrogenation is carried out in far-from-quasiequilibrium conditions under the combined effect of a stress field and a high-intensity hydrogen diffusion flow.

Experimental findings [198 – 202] indicate that the main cause of RLS in iron-based AMAs is the loss of mechanical stability at the instant of structural reorganization in the bulk sample, i.e., the transition from one metastable configuration of atoms to another (less stable) configuration. In this situation, the key factor is the additional amorphizing effect of hydrogen. At the macroscopic level, the introduction of hydrogen leads to 'fluidization' of a metal alloy, i.e., to the reduction of the effective shear modulus.

Mechanical instability resulting from such reorganization is analogous to the loss of the carrying capacity in phase transitions in a stress field (the transformation plasticity effect).

In the last decades of the twentieth century, the attention of researchers was drawn to fast-quenched alloys based on the quasibinary system TiNi – TiCu. Test samples were manufactured by the melt spinning technique to avoid formation of the brittle TiCu phase [203 – 208]. The $Ti_{50}Ni_{25}Cu_{25}$ alloy stands out from the range of similar materials due to the extreme characteristics of the martensitic transformation; it may have a crystalline, amorphous, or amorphocrystalline structure, depending on the processing mode.

Hydrogen in titanium nickelide-based alloys (e.g., in amorphous alloys based on the quasibinary system TiNi – TiCu) at 300 K has a sufficiently high diffusion coefficient ($\sim 10^{-10}$ m^2 s^{-1}) and a much greater absorption capacity than in iron-based amorphous alloys. At 300 K, these alloys can retain hydrogen rather long. Therefore, they may be used as convenient models to study the relation between the structural state and the response to hydrogen treatment, e.g., to measure variations in the shear modulus.

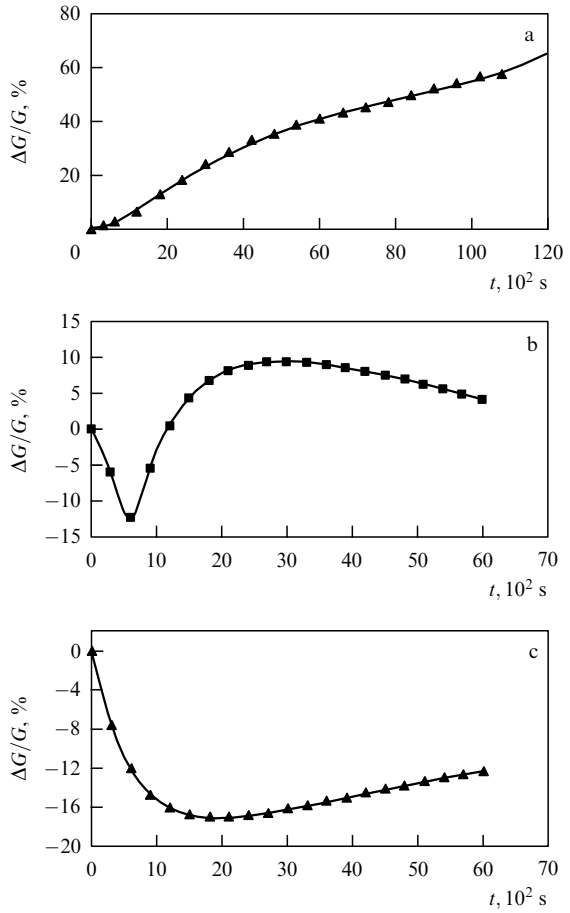

Figure 20. The effect of HS duration on the shear modulus of $Ti_{50}Ni_{25}Cu_{25}$ alloys in different structural states: (a) crystalline, (b) amorphocrystalline, and (c) amorphous ($i_c = 50$ A m^{-2}).

Figure 20 illustrates the influence of the HS duration on the shear modulus of alloys in three structural states (crystalline, amorphocrystalline, and amorphous) [209].

The increase in the shear modulus upon introduction of hydrogen in a crystalline alloy shown in Fig. 20 was observed earlier in titanium nickelide [171] but was much smaller. Hydrogen saturation significantly accelerates the mechanical after-effect and changes various physical characteristics [210 – 218]. Diffractograms are indicative of the formation of martensitic phases and the enlargement of the martensitic phase fraction after the introduction of hydrogen into crystalline and amorphocrystalline alloys of the quasibinary TiNi – TiCu system. No hydride phase was found in these experiments. Thus, hydrogen activates phase transitions leading to the appearance of the high-modulus phase characteristic of this alloy.

Hydrogen saturation of an amorphous alloy (Fig. 20c) causes a marked reduction of the shear modulus within a few minutes after its onset. X-ray diffraction studies give no evidence of new phases or the transformation of amorphous alloys into the crystalline state. The reduction in the shear modulus in this case is attributed to the superequibrium

hydrogen concentration in microvolumes of the alloy and their transition to a 'quasiliquid' state. The farther the structure of the alloy is from thermodynamic equilibrium, the greater the effect of hydrogen on the shear modulus.

In an alloy in the amorphocrystalline state (Fig. 20b), hydrogen produces two superposed effects on its crystalline and amorphous components.

The above results give experimental evidence of a change in the interatomic interaction forces at high hydrogen concentrations in materials having a disordered structure. They are of interest, bearing in mind that all theories describing the deformation and decomposition of alloys interacting with hydrogen [e.g., 17, 20 – 22, 28] a priori assume the constancy of the shear modulus entering many crucial relations. The available data point to the necessity of a sound feasibility assessment of this assumption.

8. Conclusion

The results of investigations of the synergistic effects of microplasticity in the HS of vanadium, niobium, tantalum, and zirconium indicate that active deformation starts only after the appearance of hydrides or hydride-like phases in the hydrogenated metal structure containing coexisting α- and β-phases. The formation of a hydrogen-enriched region inside a crystal is a result of hydrogen clustering facilitated by interactions involving high or superequilibrium concentrations of hydrogen. On the other hand, hydrogen clustering is nothing but a preprecipitation process related to the spinodal decay of the α-solid solution of hydrogen in a metal. The homogeneous solid solution undergoes stratification into layers with high and low hydrogen content.

It is noteworthy that iron and typical hydride-forming metals show a similar behavior under the effect of a stress field and a high-intensity hydrogen flow. The main features of this behavior are the existence of an incubation period, a nonmonotonic development of the deformation process, and a single type of the relation determining alloys' behavior at the active stage of stress relaxation and creep.

It is therefore feasible to assume that HDMA, HSR, and RMA strains in iron and metals of the Va subgroup (zirconium and palladium) undergoing HS is due to the formation of hydrides or hydrogen clusters.

A large number of observations and experimental findings available to date (see [118] for a review of the problem) allow reconsidering specific conditions for the existence of hydride-like phases, if not of iron hydride.

One of the conditions necessary for the appearance of such structures is the presence of an inhomogeneous stress field (see, e.g., Ref. [20]). In our case, the situation is complicated by the fact that electrolytic HS produces a concentration inhomogeneity. Hence, there is the possibility to regard the relevant systems of interest as open, thermodynamically nonequilibrium ones. The authors of Ref. [219] postulate a new type of spatiotemporal behavior of the systems outside the stability domain of the thermodynamic branch of states. The newly emerging (so-called dissipative) structures are essentially different from equilibrium ones obeying the Boltzmann ordering principle in that they occur only in open systems exchanging energy and mass with the ambient medium. It is this situation that is investigated in HDMA, RMA, and HSR experiments.

There is every reason to believe that the HS of iron in a stress field induces the formation of stable dissipative hydride-like structures and, in combination with other factors, promotes the development of microdeformation. Such hydride-like complexes in iron appear to have much in common with palladium hydrides and the α'-phase in Nb – H systems. Their orientation in a stress field, the development of microdistortions during the transformation, and other processes collectively make the primary cause of highly unusual, in terms of size and rate, microstrains related to direct and reverse mechanical after-effects in hydrogenated iron.

Moreover, other $M-H$ alloys in which the presence of hydride phases is beyond question and is confirmed by direct experiments are also open thermodynamically nonequilibrium systems in which microdeformations frequently develop only in the case of a continuous introduction of hydrogen or its removal from the material.

We emphasize that HS does not cause plastification of the material, i.e., enhancement of its plasticity. Conversely, treatment with hydrogen either in the presence of a stress field or without it decreases the plasticity of all studied alloys, i.e., induces the so-called hydrogen brittleness of various degrees of reversibility. The available research data give reason to argue that the degree of embrittlement in $M-H$ systems in the domain of the existence of homogeneous solid solutions decreases as this concentration range broadens. It is therefore natural that hydrogen brittleness in metals with a BBC lattice is most pronounced in iron and is less apparent in V, Nb, and Ta. In the present case, the notion of hydrogen brittleness does not imply hydride brittleness in these metals but refers only to homogeneous solid solutions (type-2 hydrogen brittleness) [20].

Strains induced by the joint action of a stress field and HS reflect a specific state of the material into which it passes as hydrogen affects the metal matrix; its introduction into an alloy prior to and during the phase transformation causes an additional reduction of the crystal lattice resistance to shear strain. It must promote phase transformations associated with the cooperative or diffusion-cooperative reorganization of the crystal lattice.

Transition of a metal alloy into a 'quasiliquid' state under conditions of structural instability and a superequilibrium concentration of hydrogen is essentially the process of crystal matrix amorphization or 'liquefaction' in separate parts of the material. It is at this juncture that catastrophic reduction of the shear modulus occurs.

Amorphization of crystalline materials at high hydrogen concentrations is known to be inherent in some crystal-type Laves phases represented by alloys of rare-earth metals with typical transition metals (Fe – Ni – Co – Zr, etc.). This phenomenon was first reported in 1983, in [25], where crystalline Zr_3Rh was studied. Interestingly, most compounds of this type undergo amorphization under the effect of hydrogen only close to the dissociation or phase transition temperature [220]. This means that two necessary conditions must be satisfied for this amorphizing effect to manifest itself: a superequilibrium hydrogen concentration and the loss of stability of the crystal lattice in advance of a phase transition of the first or second order.

We think that this fact explains the known effect described in Refs [221 – 223], i.e., the 'quasiliquid' flow of iron under its own weight during thermocycling in the hydrogen atmosphere ($P = 20$ MPa) and a transformation temperature range $\alpha \Leftrightarrow \gamma$. Experiments considered in the present review were designed according to this schedule, which included the

creation of a superequilibrium concentration of hydrogen in a metal by means of electrolytic saturation and induction (direct or indirect) of the crystal stability loss prior to the onset of phase transformations. The absence of a long-range order in the arrangement of atoms in AMA with sufficiently large hydrogen diffusion coefficients at room temperature facilitates the transition of these materials into the quasiliquid state. All experimental data available to date are consistent with the concept formulated in these works.

Thus, the synergistic effects of microplasticity in hydrogenated or deuterated Va metals, palladium and zirconium, α-iron, AMA, and TiNi-based alloys should be regarded as specific manifestations of TPE.

Despite many common features, deformations related to TPE in traditional experiments and developing in hydrogen saturation of metals in a stress field are essentially different. For example, the phase transformation is provoked by the isothermal change in the concentration of one of the components; the observed deformation effects are orders of magnitude stronger than the maximum attainable strains in thermodynamically open $M-H$ systems undergoing thermocycling in a stress field close to the phase transition temperature; and the strain rate is determined not only by specific characteristics of phase transformations and the value of the applied stress but also by the intensity of the hydrogen diffusion flow in the matrix crystal lattice and by the reduction of the effective shear modulus under the action of hydrogen (or its isotopes).

TPE is usually observed in alloys of constant composition as they are cooled (heated) near the phase transition temperature. In our case, however, the hydrogen (deuterium) concentration in the alloy is variable, while the temperature remains unaltered. This makes a fundamental difference between deformation effects in experiments on the HS of metals in a stress field and classical manifestations of the TPE allowing the introduction of the notion of the 'concentration effect of plastic transformation' (see Fig. 5). Equally important, advantageous orientations of new phase crystals for concentration TPE are not based on the temperature of crystal formation, which remains constant during the entire phase transition, but are selected in conformity with the field gradient of internal and external stresses.

Deformation due to the concentration TPE manifests itself as early as stratification of the solid solution when the 'new phase' near its concentration limit exists in the form of a hydrogen-enriched cluster because there is no interface yet as a necessary (according to Gibbs) factor for the new phase formation. Indeed, experiments on Pd and Nb have shown that the deformation in a stress field develops slightly earlier than the stable hydride phase begins to precipitate during HS (or cooling an alloy of constant composition). The greater the applied stress, the smaller are the concentrations (saturation times) at which HDMA and HSR begin to be apparent.

Thus, in all crystalline metals and alloys where the growth of HS-induced microdeformation was recorded, formation of the new hydride phase was associated with the early appearance of hydrogen-enriched clusters corresponding to solid solutions with high hydrogen content [224, 225]. These are the so-called concentration waves or concentrons [226]. At later stages, ordering of hydrogen atoms in these clusters gives rise to the hydrogen sublattice. This process is most noticeable in the HS of palladium ($\alpha \rightarrow \alpha + \beta$) and niobium ($\alpha \rightarrow \alpha + \alpha' \rightarrow \alpha + \beta$).

No synergistic effects are apparent when hydrogen interaction with a metal results in the hydride phase as a stable chemical compound with a new type of crystal lattice (e.g., in titanium).

Amorphous metal alloys, unlike their crystalline analogs, have only the short-range order in the atom arrangement. Nevertheless, the introduction of hydrogen also activates deformation processes in these alloys; some of them practically lose resistance to shear strains.

To conclude, the synergistic effects of deformation response to the introduction of hydrogen or deuterium (TPEs) into SMA, Fe, Pd, Zr, Nb, Ta, V, or TiNi are underlain by a virtually common mechanism. Superequilibrium concentration of hydrogen in the matrix crystal lattice induces structural states with low resistance to shear strain. This facilitates cooperative or diffusion-cooperative phase transformations in microvolumes oversaturated with hydrogen. Specific manifestations of MEA are reflected in the kinetic and other characteristics of the reverse mechanical after-effect, creep, and stress relaxation; they are closely related to the metal's nature and the properties of the arising hydride phases or hydride-like complexes.

Similarly to the research on the behavior of substances in electric and magnetic fields providing information about their structure, studies of the behavior of $M-H$ alloys in gradient concentration and deformation fields serve as a nontrivial and frequently the sole source of data of structural-phase transformations in thermodynamically closed and open $M-H$ systems. It may be speculated that consistent behavioral patterns of such systems in high-gradient force and concentration fields are inherent in other systems in which the high diffusibility of constituent components manifests itself only at sufficiently high temperatures.

References

1. Karpenko G V, Kripyakevich R I *Vliyanie Vodoroda na Svoistva Stali* (Influence of Hydrogen on Steel Properties) (Moscow: Metallurgizdat, 1962)
2. Śmialowski M *Hydrogen in Steel* (Oxford: Pergamon Press, 1962)
3. Cotterill P *The Hydrogen Embrittlement of Metals* (Oxford: Pergamon Press, 1961) [Translated into Russian (Moscow: Metallurgizdat, 1963)]
4. Moroz L S, Chechulin B B *Vodrodnaya Khrupkost' Metallov* (Hydrogen Brittleness of Metals) (Moscow: Metallurgiya, 1967)
5. Kolachev B A *Vodrodnaya Khrupkost' Tsvetnykh Metallov* (Hydrogen Embrittlement of Nonferrous Metals) (Moscow: Metallurgiya, 1966) [Translated into English (Jerusalem: Israel Program for Scientific Translations, 1968)]
6. Gel'd P V, Ryabov R A *Vodrod v Metallakh i Splavakh* (Hydrogen in Metals and Alloys) (Moscow: Metallurgiya, 1974)
7. Beloglazov S M *Navodorozhivanie Stali pri Elektrokhimicheskikh Protsessakh* (Electrochemical Hydrogenation of Steel) (Leningrad: Izd. LGU, 1975)
8. Maksimov E G, Pankratov O A *Usp. Fiz. Nauk* **116** 385 (1975) [*Sov. Phys. Usp.* **18** 481 (1975)]
9. Pokhmurskii V I, Shved M M, Yaremchenko N Ya *Vliyanie Vodoroda na Protsessy Deformirovaniya i Razrusheniya Zheleza i Stali* (Influence of Hydrogen on Deformation and Degradation of Iron and Steel) (Kiev: Naukova Dumka, 1977)
10. Gel'd P V, Ryabov R A, Kodes E S *Vodrod i Nesovershenstva Struktury Metallov* (Hydrogen and Metal Structure Defects) (Moscow: Metallurgiya, 1979)
11. Marichev V A *Zashchita Metallov* **16** (5) 531 (1980)
12. Hirth J P *Metal. Trans. A* **11** 861 (1980)
13. Alefeld G, Völkl J (Eds) *Hydrogen in Metals* Vol. 1 (Berlin: Springer-Verlag, 1978) [Translated into Russian, Vol. 1 (Moscow: Mir, 1981)]

14. Alefeld G, Völkl J (Eds) *Hydrogen in Metals* Vol. 2 (Berlin: Springer-Verlag, 1978) [Translated into Russian, Vol. 2 (Moscow: Mir, 1981)]
15. Shapovalov V I *Vliyanie Vodoroda na Strukturu i Svoistva Zhelezouglerodistykh Splavov* (Influence of Hydrogen on the Properties of Iron-Carbon Alloys) (Moscow: Metallurgia, 1982)
16. Birnbaum H K, in *Atom. Fract.*: *Proc. NATO Adv. Res. Inst.* (New York, 1983) p. 733, Discuss. p. 766
17. Savchenkov E A, Aitkulov P P *Korroziya Zashchita Metallov* (6) 29 (1983)
18. Oriani R A, Hirth J P, Smialowski M (Eds) *Hydrogen Degradation of Ferrous Alloys* (Park Ridge, NJ: Noyes Publ., 1985)
19. Gel'd P V, Ryabov R A, Mokhracheva L P *Vodorod i Fizicheskie Svoistva Metallov i Splavov*: *Gidridy Perekhodnykh Metallov* (Hydrogen and Physical Properties of Metals and Alloys: Hydrides of Transition Metals) (Moscow: Nauka, 1985)
20. Kolachev B A *Vodrodnaya Khrupkost' Metallov* (Hydrogen Brittleness of Metals) (Moscow: Metallurgiya, 1985)
21. Archakov Yu I *Vodorodnaya Korroziya Metallov* (Hydrogen-Mediated Corrosion of Metals) (Moscow: Metallurgiya, 1985)
22. Shved M M *Izmenenie Ekspluatatsionnykh Svoistv Zheleza i Stali pod Vliyaniem Vodoroda* (Changes of Operational Properties of Iron and Steel Under Effect of Hydrogen) (Kiev: Naukova Dumka, 1985)
23. Nosov V K, Kolachev B A *Vodorodnoe Plastifitsirovanie pri Goryachei Deformatsii Titanovykh Splavov* (Hydrogen-Assisted Plastification in Hot Deformation of Titanium Alloys) (Moscow: Metallurgiya, 1986)
24. Ageev V N et al. *Vzaimodeistvie Vodoroda s Metallami* (Hydrogen Interaction with Metals) (Executive Ed. A P Zakharov) (Moscow: Nauka, 1987)
25. Fukai Y *The Metal–Hydrogen System*: *Basic Bulk Properties* (Berlin: Springer-Verlag, 1993)
26. Spivak L V, Skryabina N E, Kats M Ya *Vodorod i Mekhanicheskoe Posledeistvie v Metallakh i Splavakh* (Hydrogen and Mechanical Aftereffects in Metals and Alloys) (Perm': Izd. PGU, 1993)
27. Beloglazov S M *Elektrokhimicheskii Vodorod i Metally*: *Povedenie, Bor'ba s Okhrupchivaniem* (Electrochemical Hydrogenation of Metals: Behavior, Control of Embrittlement) (Kaliningrad: Izd. Kaliningradskogo Gos. Univ., 2004)
28. Goltsov V A (Ed.) *Progress in Hydrogen Treatment of Materials* (Donetsk: Coral Gables Kassiopeya Ltd, 2001)
29. Nechaev Yu S˚ *Usp. Fiz. Nauk* **171** 1251 (2001) [*Phys. Usp.* **44** 1189 (2001)]
30. *3rd Intern. Conf.* "*Hydrogen Treatment of Materials*" (*HTM-2001*), *Donetsk–Mariupol, May 14–18, 2001*, Abstracts Book
31. *2nd Intern. Conf. on Environmental Degradation of Engineering Materials, EDEM'2003, 30 June–3 July 2003, Bordeaux, France*, Abstracts Book
32. *2nd Intern. Workshop* "*Interaction of Hydrogen Isotopes with Structural Materials*", *12–16 April, 2004, Sarov, Russia*, Abstracts Book
33. *Intern. Symp. on Metal–Hydrogen Systems*: *Fundamentals and Applications, 5–10 Sept., 2004, Krakow, Poland*, Abstracts Book
34. *2nd Intern. Symp. on Hydrogen in Matter* (*ISOHIM*), *13–17 June, 2005, Uppsala, Sweden*, Abstracts Book
35. *3rd Intern. Conf. on Environmental Degradation of Engineering Materials, EDEM'2007, 21–24 May, 2007, Gdańsk–Jastrzebia Góra, Poland*, Abstracts Book
36. Galland I, Azou P, Bastien P *C.R. Acad. Sci. C* (Paris) **268** 27 (1969)
37. Asano S, Otsuka R *Scripta Met.* **10** 1015 (1976)
38. Lunarska E et al. *Scripta Met.* **17** 705 (1983)
39. Flis J, Janko A *Bull. Acad. Polon. Sci. Ser. Sci. Chim.* **12** (1) 17 (1982)
40. Flis J *Bull. Acad. Polon. Sci. Ser. Sci. Chim.* **12** 809 (1964)
41. Flis J, Smialowski M *Scripta Met.* **13** 641 (1979)
42. Lunarska E, Wokulski Z *Acta Met.* **30** 2173 (1982)
43. Lunarska E *Wplyw Wodoru na Plastyczne Wlasnosci Zelaza* (Zeszyty Nauk Akad. Gorniczo-Hutnicza, No. 997, Met. Odlewnictwo, No. 101) (Krakow, 1984) p. 66
44. Kimura A, Matsui H, Kimura H *Trans. Jpn. Inst. Met. Suppl.* **21** 541 (1980)
45. Park C G et al. *Scripta Met.* **14** 279 (1980)
46. Kimura A, Birnbaum H K *Scripta Met.* **21** 53 (1987)
47. Tabata T, Birnbaum H K *Scripta Met.* **18** 231 (1984)
48. Tabata T *Bull. Jpn. Inst. Met.* **24** 485 (1985)
49. Hagi H, Hayashi Y, Ohtani N *J. Jpn. Inst. Met.* **42** (2) 124 (1978)
50. Hagi H, Hayashi Y *J. Soc. Mater. Sci. Jpn.* **37** 1442 (1988)
51. Zakrochimski T *Zashchita Metallov* **19** 733 (1983)
52. Lee J-L, Lee J-Y *J. Mater. Sci.* **22** 3939 (1987)
53. Choo W Y *J. Mater. Sci.* **19** 2633 (1984)
54. Gel'd P V et al. *Dokl. Akad. Nauk SSSR* **261** 660 (1981)
55. Gel'd P V et al. *Dokl. Akad. Nauk SSSR* **267** 659 (1982)
56. Spivak L V et al. *Fiz. Met. Metalloved.* **58** 1215 (1984)
57. Skryabina N E et al. *Izv. Akad. Nauk SSSR Metally* (1) 145 (1984)
58. Aizentson E G et al. *Izv. Vyssh. Uchebn. Zaved. Chernaya Metallurgiya* (8) 74 (1985)
59. Aizentson E G et al. *Izv. Vyssh. Uchebn. Zaved. Chernaya Metallurgiya* (4) 76 (1985)
60. Spivak L V, Skryabina N E *Fiz. Met. Metalloved.* **60** 1037 (1985)
61. Spivak L V, Skryabina N E, Kuznetsova E V *Fiz. Met. Metalloved.* **61** 205 (1986)
62. Kats M Ya, Skryabina N E *Pis'ma Zh. Tekh. Fiz.* **12** 21 (1986) [*Sov. Tech. Phys. Lett.* **12** 9 (1986)]
63. Gel'd P V, Kats M Ya, Spivak L V *Dokl. Akad. Nauk SSSR* **286** 106 (1986)
64. Gel'd P V, Kats M Ya, Spivak L V *Fiz. Met. Metalloved.* **64** 406 (1987)
65. Gel'd P V et al. *Fiz. Met. Metalloved.* **65** 114 (1988)
66. Spivak L V, Skryabina N E *Mekhanizmy Uprocheniya i Svoistva Metallov* (Mechanisms of Strengthening and Properties of Metals) (Executive Ed. S A Golovin) (Tula: Izd. TPI, 1988) p. 61
67. Kats M Ya, Spivak L V *Zh. Tekh. Fiz.* **59** (2) 196 (1989) [*Sov. Phys. Tech. Phys.* **34** 252 (1989)]
68. Spivak L V et al. *Fiz. Met. Metalloved.* (6) 142 (1991)
69. Spivak L V, Kats M Ya *Izv. Akad. Nauk SSSR Metally* (1) 189 (1992)
70. Spivak L V, Skryabina N E *Fiz. Met. Metalloved.* **76** (5) 141 (1993)
71. Spivak L V *Izv. Vyssh. Uchebn. Zaved. Chernaya Metallurgiya* (8) 52 (1993)
72. Skryabina N E, Spivak L V *Fiz. Met. Metalloved.* **79** (4) 87 (1995)
73. Spivak L V, Skryabina N E *Mezhdunar. Nauchn. Zh.* '*Al'ternativnaya Energetika i Ekologiya*' (1) 176 (2003)
74. Skryabina N E, Spivak L V *Izv. Ross. Akad. Nauk Ser. Fiz.* **67** 1411 (2003)
75. Spivak L V, Skryabina N E *Mezhdunar. Nauchn. Zh.* '*Al'ternativnaya Energetika i Ekologiya*' (3) 85 (2000)
76. Kuz'min S L et al. *Fiz. Met. Metalloved.* **57** 612 (1984)
77. Likhachev V A *Izv. Vyssh. Uchebn. Zaved. Fiz.* (5) 20 (1985) [*Sov. Phys. J.* **28** 355 (1985)]
78. Likhachev V A, Kuz'min S L, Kamentseva Z P *Effekt Pamyati Formy* (Shape Memory Effect) (Leningrad: Izd. LGU, 1987)
79. Likhachev V A, Patrikeev Yu I, Shupletsov V N *Fiz. Met. Metalloved.* **61** 121 (1986)
80. Andrievskii R A *Materialovedenie Gidridov* (Science of Hydrides) (Moscow: Metallurgiya, 1986)
81. Mueller W M, Blackledge J P, Libowitz G G (Eds) *Metal Hydrides* (New York: Academic Press, 1968) [Translated into Russian (Moscow: Atomizdat, 1973)]
82. Antonova M M *Svoistva Gidridov Metallov*. Spravochnik (Properties of Metal Hydrides. Reference Book) (Kiev: Naukova Dumka, 1975)
83. Andrievskii R A, Umanskii Ya S *Fazy Vnedreniya* (Interstitial Phases) (Moscow: Nauka, 1977)
84. Muetterties E L (Ed.) *Transition Metal Hydrides* (New York: M. Dekker, 1971) [Translated into Russian (Moscow: Mir, 1975)]
85. Goldschmidt H J *Interstitial Alloys* (New York: Plenum Press, 1967) [Translated into Russian (Moscow: Mir, 1971)]
86. Dotsenko V I "Relaksatsiya napryazhenii v kristallakh" ("Stress relaxation in crystals"), Preprint No. 1 (Khar'kov: Fiz.-Tekh. Inst. Nizkikh Temperatur AN USSR, 1979)
87. Butt M Z, Sani M Y *J. Natur. Sci. Math.* **26** (2) 69 (1986)
88. Mazzolai F M *Z. Phys. Chem.* **145** (1–2) 199 (1985)
89. Bilenko I A et al. *Vestn. Mosk. Gos. Univ. Ser. Fiz. Astron.* **30** (5) 90 (1989)
90. Bonneville J *Rev. Phys. Appl.* **23** 677 (1988)
91. Paterson M S *Mech. Mater.* **2** 103 (1983)

92. Abramova A P et al. *Metallofiz*. **8** (2) 28 (1986)
93. Larikov L N, Isaichev V I *Diffuziya v Metallakh i Splavakh* (Diffusion in Metals and Alloys) (Ser. 'Struktura i Svoistva Metallov i Slpavov') (Structure and Properties of Metals and Alloys) (Kiev: Naukova Dumka, 1987)
94. Spivak L V, Skryabina N E *Pis'ma Zh. Tekh. Fiz*. **21** (1) 20 (1995) [*Tech. Phys. Lett*. **21** 8 (1995)]
95. Spivak L V, Skryabina N E *Fiz. Met. Metalloved*. **81** (5) 165 (1996)
96. Flanagan T B, Schober T, Wenzl H *Acta Met*. **33** 685 (1985)
97. Peshcherenko M P, Spivak L V *Vestn. Perm. Univ. Ser. Fiz*. (5) 24 (1999)
98. Gol'tsov V A, Machikina I Yu, Timofeev N I *Fiz. Met. Metalloved*. **50** 1299 (1980)
99. Skryabina N E, Spivak L V, Timofeev N I *Fiz. Met. Metalloved*. **64** 1038 (1987)
100. Spivak L V et al. *Fiz. Met. Metalloved*. **64** 798 (1987)
101. Spivak L V, Skryabina N E *Fiz. Met. Metalloved*. **91** (4) 63 (2001) [*Phys. Met. Metallogr*. **91** 383 (2001)]
102. Goltsov V A et al., in *Progress in Hydrogen Treatment of Materials* (Ed. V A Goltsov) (Donetsk: Coral Gables Kassiopeya Ltd, 2001) p. 95
103. Gol'tsov V A, Red'ko A L, Glukhova Zh L *Fiz. Met. Metalloved*. **95** (1) 21 (2003) [*Phys. Met. Metallogr*. **95** 17 (2003)]
104. Gol'tsov V A, Glukhova Zh L *Fiz. Met. Metalloved*. **90** (4) 68 (2000) [*Phys. Met. Metallogr*. **90** 382 (2000)]
105. Goltsov V A, Vlasenko N B, in *Progress in Hydrogen Treatment of Materials* (Ed. V A Goltsov) (Donetsk: Coral Gables Kassiopeya Ltd, 2001) p. 203
106. Puzanova I M et al. *Izv. Vyssh. Uchebn. Zaved. Fiz*. (11) 7 (1979) [*Sov. Phys. J*. **22** 1129 (1979)]
107. Bucur R V *Surf. Coat. Technol*. **28** 413 (1986)
108. Kleperis J J et al. *Phys. Status Solidi A* **81** K121 (1984)
109. Wicke E, Blaurock J *J. Less Common Met*. **130** 351 (1987)
110. Spivak L V, Skryabina N E *Pis'ma Zh. Tekh. Fiz*. **20** (16) 20 (1994) [Spivak L V, Skryabina N E *Tech. Phys. Lett*. **20** 653 (1994)]
111. Choo W Y *J. Iron Steel Inst. Jpn*. **70** 1442 (1984)
112. Okrainets P M, Pishchak V K *Metallofiz*. **7** (3) 73 (1985)
113. Bystrov L N, Tsepelev A B *Izv. Akad. Nauk SSSR Metally* (4) 171 (1984)
114. Tien J K, Yen C T *Adv. Criog. Eng*. **30** 319 (1983)
115. Bonneville J *Rev. Phys. Appl*. **23** 677 (1988)
116. Lepin G F *Polzuchest' Metallov i Kriterii Zharoprochnosti* (Creep in Metals and Criteria for Heat Resistance) (Moscow: Metallurgiya, 1976)
117. Čadek J *Creep Kovových Materiálú* (Praha: Academia, 1984) [Translated into English: *Creep in Metallic Materials* (Amsterdam: Elsevier, 1988); Translated into Russian (Moscow: Mir, 1987)]
118. Spivak L V, Skryabina N E *Fiz. Met. Metalloved*. **58** 200 (1984)
119. Tanabe T, Yamanishi Y, Imoto S *Trans. Jpn. Inst. Met*. **2** (1) 1 (1984)
120. Gupta I, Li J C M *Met. Trans*. **1** 2323 (1970)
121. Smialowski M *Scripta Met*. **13** 393 (1979)
122. Oriani R A, Josephic P H *Met. Trans*. **11** 1803 (1980)
123. Oriani R A, in *Atom. Fract.: Proc. NATO Adv. Res. Sust*. (New York, 1983) p. 795
124. Volke J, in *Metal Hydrides*: *Proc. NATO Adv. Study Inst*. (New York, 1981) p. 105
125. Kubashevski O *Diagrammy Sostoyaniya Dvoinykh System na Osnove Zheleza* (Diagram of the State of Iron-Based Binary Systems) (Moscow: Metallurgiya, 1985)
126. Zav'yalov A S *Izv. Vyssh. Uchebn. Zaved. Chernaya Metallurgiya* (1) 102 (1986)
127. Kripyakevich V N et al. *Fiziko-Khimicheskaya Mekhanika Materialov* **7** (3) 60 (1971)
128. Lange K W, Konig N J *Forschungsber. Landes Nordrhein-Westfalen* (2566) 66 (1976)
129. Choo W Y et al. *J. Mater. Sci*. **16** 1285 (1981)
130. Vasilenko N I et al. *Fiziko-Khimicheskaya Mekhanika Materialov* **18** (3) 16 (1982)
131. Yamanishi Y et al. *Trans. Jpn. Inst. Met*. **24** (1) 49 (1983)
132. Schurmann E et al. *Stel. Res*. **57** (11) 546 (1986)
133. Spivak L V, Skryabina N E *J. Adv. Mater*. (2) 147 (1995)
134. Isakov M G, Izotov V I, Filippov G A *Fiz. Met. Metalloved*. **90** (4) 105 (2000) [*Phys. Met. Metallogr*. **90** 418 (2000)]
135. Izotov V I, Pozdnyakov V A, Filippov G A *Fiz. Met. Metalloved*. **91** (5) 84 (2001) [*Phys. Met. Metallogr*. **91** 509 (2001)]
136. Hirth J P, Carnahan B *Acta Met*. **26** 1795 (1978)
137. Wang Y-B, Chu W-Y, Hsiao C-M *Scripta Met*. **19** 1161 (1985)
138. Zhang T-Y, Chu W-Y, Hsiao C-M *Scripta Met*. **20** 225 (1986)
139. Li J C M, Park C G, Ohr S M *Scripta Met*. **20** 371 (1986)
140. Li J C M et al. *Scripta Met*. **21** 1595 (1987)
141. Rodríguez M V, Ficalora P J *Scripta Met*. **20** 615 (1986)
142. Rodríguez M V, Ficalora P J *Mater. Sci. Eng*. **85** 43 (1987)
143. Bondarenko I E, Nikitenko V I, in *Problemy Prochnosti i Plastichnosti Tverdykh Tel* (Problems in Strength and Plasticity of Solids) (Executive Ed. S N Zhukov) (Leningrad: Nauka, 1979) p. 244
144. Mikitishin S I *Fiziko-Khimicheskaya Mekhanika Materialov* **20** (3) 23 (1984)
145. Fishgoit A V, Kolachev B A, in *Vzaimodeistvie Defektov Kristallicheskoi Reshetki i Svoistva Metallov* (Interaction of Crystal Lattice Defects and Properties of Metals) (Executive Ed. S A Golovin) (Tula: TPU, 1984) p. 3
146. Troitskii O A, Kalymbetov P U *Izv. Akad. Nauk SSSR Metally* (3) 85 (1981)
147. Troitskii O A, Kalymbetov P U *Fiz. Met. Metalloved*. **51** 1056 (1981)
148. Spitsyn V I, Troitskii O A *Elektroplasticheskaya Deformatsiya Metallov* (Electroplastic Deformation of Metals) (Moscow: Nauka, 1985)
149. Tabata T, Birnbaum H K *Scripta Met*. **17** 947 (1983)
150. Matsui H *Bull. Jpn. Inst. Met*. **23** (16) 425 (1984)
151. Robertson I M, Birnbaum H K *Scripta Met*. **18** 269 (1984)
152. Robertson I M, Birnbaum H K *Asta Met*. **34** 353 (1986)
153. Robertson I M et al. *Scripta Met*. **18** 841 (1984)
154. Spivak L V *Izv. Vyssh. Uchebn. Zaved. Chernaya Metallurgiya* (8) 52 (1993)
155. Kats M Ya, Spivak L V, in *Vnutrennee Trenie i Dislokatsionnaya Struktura Metallov* (Internal Friction and Dislocation Structure of Metals) (Executive Ed. S A Golovin) (Tula: TPI, 1990) p. 83
156. Lotkov A I, Grishkov V N *Izv. Vyssh. Uchebn. Zaved. Fiz*. **28** (5) 68 (1985) [*Sov. Phys. J*. **28** 390 (1985)]
157. Fedotov S G *Dokl. Akad. Nauk SSSR* **270** 625 (1983)
158. Pushin V G et al. *Fiz. Met. Metalloved*. **66** 350 (1988)
159. Kondrat'ev V V et al. *Fiz. Met. Metalloved*. **66** 359 (1988)
160. Asaoka T et al. *J. Inst. Ind. Sci. Univ. Tokyo* **38** (11) 497 (1986)
161. Schmidt R et al. *J. Phys.: Condens. Matter* **1** 2473 (1989)
162. Chao J et al., in *Hydrogen Systems*: *Intern. Symp., Beijing, China, 7–11 May, 1985, Papers* Vol. 1 (Eds D Nejat Veziroğlu, Z Yajie, B Deyou B) (Elmsford, NY: Pergamon Press, 1986) p. 445
163. Stepanov I A, Flomenblit Yu M, Zaimovskii V A *Fiz. Met. Metalloved*. **55** 612 (1983)
164. Shorshorov M Kh et al. *Fiz. Met. Metalloved*. **60** 326 (1985)
165. Shorshorov M Kh et al. *Dokl. Akad. Nauk SSSR* **283** 370 (1985) [*Sov. Phys. Dokl*. **30** 611 (1985)]
166. Shorshorov M Kh et al. *Fiz. Met. Metalloved*. **64** 498 (1987)
167. Maslenkov S B et al. *Metalloved. Termicheskaya Obrabotka Mater*. (10) 6 (1988)
168. Shorshorov M Kh et al. *Fiz. Met. Metalloved*. **66** 307 (1988)
169. Adachi Y et al. *J. Jpn. Inst. Met*. **54** 525 (1990)
170. Spivak L V *Vestn. Perm. Univ. Ser. Fiz*. (4) 171 (1994)
171. Spivak L V, Skryabina N E, Khachin V N *Fiz. Met. Metalloved*. **79** (4) 138 (1995) [*Phys. Met. Metallogr*. **79** 450 (1995)]
172. Libowitz G G, Maeland A J *J. Less Common Met*. **101** 131 (1984)
173. Maeland A J, in *Rapidly Quenched Metals*: *Proc. of the 5th Intern. Conf., Würzhurg, Germany, Sept. 3–7, 1984* Vol. 2 (Eds S Steeb, H Warlimont) (Amsterdam: North-Holland, 1985) p. 1507
174. Roshchupkin V V et al., in *Teplofizika Kondensirovannykh Sred* (Thermophysics of Condensed Media) (Executive Ed. I I Novikov) (Moscow: Nauka, 1985) p. 95
175. Koster U, Schroeder H, in *Glass — Current Issues* (Proc. NATO ASI, Ser. E, No. 92, Eds A F Wright, J Dupuy) (Dordrecht: Martinus Nijhoff Publ., 1985) p. 86
176. Chambron A, in *Rapidly Quenched Metals*: *Proc. of the 5th Intern. Conf., Würzburg, Germany, Sept. 3–7, 1984* Vol. 2 (Eds S Steeb, H Warlimont) (Amsterdam: North-Holland, 1985) p. 1549
177. Kirchheim R *Acta Met*. **30** 1069 (1982)

178. Flis J et al. *Acta Met*. **35** 2071 (1987)
179. Spivak L V, Khonik V A, Skryabina N E *Zh. Tekh. Fiz*. **65** (5) 104 (1995) [*Tech. Phys*. **40** 463 (1995)]
180. Khonik V A, Spivak L V *Acta. Mater*. **44** 367 (1996)
181. Skryabina N E, Spivak L V *Vestn. Perm. Univ. Ser. Fiz*. (4) 171 (1995)
182. Monokhin A I et al. *Amorfnye Splavy* (Amorphous Alloys) (Moscow: Metallurgiya, 1987)
183. Sudzuki K, Fudzimori H, Hasimoto K *Amorphous Metals* [Translated into Russian from Japanese (Moscow: Metallurgiya, 1987)]
184. Skryabina N E *Pis'ma Zh. Tekh. Fiz*. **22** (23) 36 (1996) [*Tech. Phys. Lett*. **22** 965 (1996)]
185. Skryabina N E et al. *Fiz. Met. Metalloved*. **83** (3) 139 (1997) [*Phys. Met. Metallogr*. **83** 331 (1997)]
186. Khominskii M A et al. *Vestn. Perm. Univ. Ser. Fiz*. (4) 3 (1998)
187. Skryabina N E, Petrov A S *Vestn. Perm. Univ. Ser. Fiz*. (4) 21 (1998)
188. Spivak L V, Skryabina N Ye *Int. J. Hydrogen Energy* **24** 795 (1999)
189. Skryabina N E et al. *Pis'ma Zh. Tekh. Fiz*. **26** (21) 26 (2000) [*Tech. Phys. Lett*. **26** 947 (2000)]
190. Kinev A S et al. *Mezhdunar. Nauchn. Zh.* '*Al'ternativnaya Energetika i Ekologiya*' **1** 174 (2000)
191. Skryabina N E et al. *Materialovedenie* (6) 29 (2001)
192. Brechko T M et al. *Pis'ma Zh. Tekh. Fiz*. **30** (9) 68 (2004) [*Tech. Phys. Lett*. **30** 383 (2004)]
193. Berry B S, Pritchet W C *J. Appl. Phys*. **52** 1865 (1981)
194. Berry B S, Pritchet W C *Phys. Rev. B* **24** 2299 (1981)
195. Berry B S, Pritchet W C *Z. Phys. Chem. Neue Folge* **163** 381 (1989)
196. Pavlov V V *O* '*Krizise*' *Kineticheskoi Teorii Zhidkosti i Zatverdevaniya* (On the 'Crisis' of Kinetic Theory of Liquid and Solidification) (Ekaritenburg: Ural'skaya Gos. Gorno-Geologicheskaya Akademiya, 1997)
197. Polukhin V A, in *Stroenie i Svoistva Metallicheskikh i Shlakovykh Rasplavov*: *IX Vseross. Konf., Ekaterinburg* (Structure and Properties of Metallic and Slag Melts) Vol. 1 (1989) p. 19
198. Skryabina N E, Spivak L V *Izv. Ross. Akad. Nauk Ser. Fiz*. **65** 1384 (2001) [*Bull. Russ. Acad. Sci., Phys*. **65** 1574 (2001)]
199. Spivak L V *Sorosovskii Obrazovatel'nyi Zh*. (10) 108 (1999)
200. Skryabina N E, Spivak L V *Vestn. Perm. Univ. Ser. Fiz*. (6) 13 (2000)
201. Skryabina N, Spivak L *J. Alloys Compounds* **356 – 357** 630 (2003)
202. Skryabina N et al. *J. Metastable Nanocryst. Mater*. **20 – 21** 517 (2004)
203. Matveeva N M et al. *Izv. Akad. Nauk SSSR Metally* (4) 171 (1989)
204. Rösner H et al. *Mater. Sci. Eng. A* **273 – 275** 733 (1999)
205. Shelyakov A V et al., in *Shape Memory Alloys*: *Fundamentals, Modelling and Industrial Applications* (Eds F Trochu, V Brailovski, A Galibois) (Warrendale, PA: Minerals, Metals, & Materials Soc., 1999) p. 295
206. Vintaikin E Z et al. *Fiz. Met. Metalloved*. **90** (4) 85 (2000) [*Phys. Met. Metallogr*. **90** 398 (2000)]
207. Rösner H et al. *Acta Mater*. **49** 1541 (2001)
208. Potapov P L, Shelyakov A V, Schryvers D *Scripta Mater*. **44** (1) 1 (2001)
209. Skryabina N E, Spivak L V, Shelyakov A V *Pis'ma Zh. Tekh. Fiz*. **30** (7) 25 (2004) [*Tech. Phys. Lett*. **30** 270 (2004)]
210. Spivak L V et al. *Pis'ma Zh. Tekh. Fiz*. **30** (19) 1 (2004) [*Tech. Phys. Lett*. **30** 799 (2004)]
211. Spivak L V et al. *Izv. Ross. Akad. Nauk Ser. Fiz*. **69** 1302 (2005) [*Bull. Russ. Acad. Sci., Phys*. **69** 1459 (2005)]
212. Spivak L V et al. *Vestn. Perm. Univ. Ser. Fiz*. (1) 21 (2005)
213. Spivak L V et al. *Vestn. Perm. Univ. Ser. Fiz*. (1) 17 (2005)
214. Spivak L V at al. *Fundamental'nye Problemy Sovremennogo Materialovedeniya* **2** (2) 105 (2005)
215. Skryabina N E et al. *Vestn. Perm. Univ. Ser. Fiz*. (1) 83 (2006)
216. Spivak L V et al. *Mezhdunar. Nauchn. Zh.* '*Al'ternativnaya Energetika Ekologiya*' (1) 37 (2007)
217. Spivak L V et al. *Vestn. Perm. Univ. Ser. Fiz*. (1) 106 (2007)
218. Spivak L V, Skryabina N E *Izv. Vyssh. Uchebn. Zaved. Chernaya Metallurgiya* (4) 43 (1991)
219. Nicolis G, Prigogine I *Self-Organization in Nonequilibrium Systems* (New York: Wiley, 1977) [Translated into Russian (Moscow: Mir, 1979)]
220. Aoki K, in *Progress in Hydrogen Treatment of Materials* (Ed. V A Goltsov) (Donetsk: Coral Gables. Kassiopeya Ltd, 2001) p. 353
221. Shapovalov V I, Grigorovich V I *Dokl. Akad. Nauk SSSR* **267** 877 (1982)
222. Shapovalov V I, Karpov V Yu *Fiz.-Khim. Mekh. Mater*. **18** (3) 38 (1982)
223. Shapovalov V I, Karpov V Yu *Fiz. Met. Metalloved*. **55** 805 (1983)
224. Khachaturyan A G *Teoriya Fazovykh Prevrashchenii i Struktura Tverdykh Rastvorov* (The Theory of Phase Transformations and Structure of Solid Solutions) (Moscow: Nauka, 1974)
225. Ustinovshchikov Yu I, Pushkarev B E *Usp. Fiz. Nauk* **176** 611 (2006) [*Phys. Usp*. **49** 593 (2006)]
226. Katsnel'son A A, Olemskoi A I *Mikroskopicheskaya Teoriya Neodnorodnykh Struktur* (Microscopic Theory of Inhomogeneous Structures) (Moscow: Izd. MGU, 1987)